Archives of Computational Methods in Engineering
https://doi.org/10.1007/s11831-025-10318-4

REVIEW

Machine Learning for Underwater Explosion Prediction: A Comprehensive Review of Methods, Challenges and Future Directions

Jacopo Bardiani[1] · **Claudio Sbarufatti**[1] · **Andrea Manes**[1]

Received: 2 May 2025 / Accepted: 15 July 2025

Abstract
Underwater explosions (UNDEX) represent a critical threat to the structural integrity of submerged and floating systems across marine, offshore, and civil engineering sectors. Simulating their complex effects—driven by strong fluid–structure interaction (FSI), cavitation, and nonlinear material behavior—typically relies on numerical methods that, although accurate, are computationally expensive and not ideal for rapid predictions in practical scenarios. To overcome these limitations, the integration of Artificial Intelligence (AI) and Machine Learning (ML) into UNDEX research has recently emerged as a promising, albeit still developing, alternative. This paper presents a systematic review of AI and ML applications for predicting structural and fluid responses under underwater blast loading, focusing on developments over the past two decades. After introducing the governing physics of UNDEX events and summarizing the numerical techniques commonly used for dataset generation, the paper provides a detailed analysis of existing AI and ML approaches for UNDEX prediction. Despite the relative novelty of this research field, the paper concludes by highlighting the main challenges and proposing future research directions, including the adoption of advanced learning paradigms tailored to UNDEX scenarios. Practical guidelines are also offered to support future efforts in developing ML-based frameworks for accurate and efficient UNDEX response prediction.

1 Introduction

Understanding the dynamic response of submerged and partially submerged structures subjected to pressure loads is of fundamental importance across several engineering domains, including naval architecture, offshore engineering, and civil infrastructure. These structures often operate in harsh environments where they are exposed to extreme dynamic events. Among the various sources of pressure loading, underwater explosions (UNDEX) represent one of the most severe threats due to the rapid pressure rise and strong fluid–structure interaction they generate. Such events can severely compromise the structural integrity and operational capability of a wide range of systems, including submarines, cargo and combat vessels, offshore oil platforms, and large-scale hydraulic structures such as dams, locks, and coastal protection systems. Accurately modeling and assessing the effects of UNDEX events is therefore essential to ensure the safety, resilience, and continued functionality of these critical structures.

A typical UNDEX event can generate three distinct damage mechanisms that affect a structure, depending on the distance between the explosion and the hull [1–3]. Initially, a high-intensity primary shock wave is produced, which travels through the water at high velocity and impacts the structure with an abrupt and intense pressure front, potentially causing immediate local damage [4]. This is followed by a secondary phase characterized by low-frequency pressure oscillations, resulting from the pulsation of the gas bubble generated by the explosion [5, 6]. These oscillations can resonate with the structural modes of the system, leading to significant global vibrations and potential fatigue damage. Finally, as the gas bubble collapses, high-speed water jets may be produced [7], which can exert localized pressure and impact forces on the structure, further compromising its integrity. The combined effect of these mechanisms poses a complex challenge in the design and analysis of submerged and floating structures, especially in safety–critical applications.

✉ Jacopo Bardiani
jacopo.bardiani@polimi.it

[1] Politecnico di Milano, Department of Mechanical Engineering, Via G. La Masa 1, 20156 Milan, Italy

Published online: 21 July 2025

The three mechanisms previously mentioned give rise to highly complex physical phenomena, primarily due to the strong coupling between fluid and structural domains, commonly referred to as fluid–structure interaction (FSI) [8, 9]. These interactions are further complicated by large structural deformations, potential fracturing and failure processes, and pronounced material nonlinearities driven by high strain rates and elevated temperatures [10–12]. In contrast to explosions occurring in air, UNDEX events introduce a distinct set of challenges due to the properties of the underwater medium [13]. The resulting FSI can trigger a range of interconnected effects, such as cavitation near the surface of the structure, reflection of pressure waves at fluid–structure boundaries, and partial absorption of energy by the structure [14–18]. These coupled phenomena significantly influence both the local and global dynamic response of the system, making accurate modeling and prediction particularly demanding [19].

UNDEX are generally classified based on the proximity of the structure to the explosion site, particularly with respect to the influence zone of the gas bubble. Two main categories are typically identified [2, 10, 20–22]: contact explosions, where the explosive charge is in direct contact with the structure, and non-contact explosions, where the charge detonates at a certain distance from the target. Non-contact explosions can be further divided into near-field and far-field scenarios, depending on the stand-off distance. In far-field UNDEX, for example, the stand-off distance exceeds the maximum radius reached by the gas bubble during its initial pulsation cycle [23]. This distinction is crucial, as the intensity and nature of the loading mechanisms acting on the structure vary significantly across these categories.

Three primary approaches are commonly employed to investigate UNDEX and their effects on structures [24–27]: experimental testing, analytical modeling, and numerical simulation. These methodologies aim to characterize both the nature of the pressure loading generated by UNDEX events and the resulting nonlinear dynamic responses of affected structures.

Experimental investigations of UNDEX are inherently challenging due to the complex and hazardous nature of the phenomena [28, 29]. In addition to safety concerns, the high costs and logistical difficulties associated with such tests—particularly at full scale—often make them impractical [24]. While scaled experiments can offer valuable approximations of real behavior, the limited availability and dissemination of experimental data significantly constrain the broader understanding and validation of UNDEX-related responses [30].

Analytical models play a fundamental role in the study of UNDEX phenomena, offering valuable theoretical insight into the potential effects and consequences of such events. However, their applicability is often constrained by the simplifying assumptions required to make the problem tractable [3, 24]. As a result, these models may fall short in accurately capturing the full complexity of the physical interactions involved in real-world scenarios [31–33].

As a result of continuous advancements in numerical methods and computational capabilities, it is now possible to perform highly detailed simulations of UNDEX events using high-performance computing systems [20, 27, 34]. State-of-the-art simulation software—such as LS-DYNA, ABAQUS, ANSYS, and MSC DYTRAN—is widely employed to model the transient pressure loads and resulting structural responses associated with UNDEX across a broad range of engineered systems, including marine, offshore, and civil infrastructure [24, 35–42].

Various numerical strategies can be adopted to simulate UNDEX events; however, the most prominent distinction lies between coupled and uncoupled methodologies, with coupled approaches being the most widely used in recent years [43–45]. Coupled methods simultaneously solve the interaction between the pressure wave generated by the explosion and the dynamic structural response of the hull within a unified computational framework, ensuring a more accurate representation of FSI [46, 47]. In contrast, uncoupled approaches treat the fluid and structural domains separately, typically following a sequential two-step procedure that does not directly capture the mutual interaction during the event [48].

Coupled numerical approaches used to address transient FSI problems in UNDEX scenarios can be further categorized into three main strategies, depending on how the fluid and structural domains are represented [9, 24]: Eulerian–Eulerian (E–E), Lagrangian–Lagrangian (L–L), and Eulerian–Lagrangian (E–L). The E–E methods treats both fluid and structure within an Eulerian framework, but due to its unsuitability for solid dynamics, it has not been adopted in numerical studies to date [24]. Inside the E–L group, the most employed techniques are the Coupled Eulerian–Lagrangian (CEL) and the Arbitrary Lagrangian–Eulerian (ALE) methods [38, 49]. While CEL allows the fluid to flow through a fixed mesh (Eulerian) and the structure to deform following the mesh (Lagrangian), ALE enables mesh motion to partially follow the material, offering a compromise that reduces mesh distortion during large deformations. Both methods provide effective tools for capturing complex FSI phenomena in UNDEX simulations [36, 50–52]. In addition, the most used L–L method for UNDEX simulations is the Coupled Acoustic-Structural Approach (CASA) [33, 53–57]. While traditionally applied in acoustic problems, CASA has been effectively used to study UNDEX scenarios by modeling the fluid with Lagrangian acoustic elements—defined by a single pressure degree of freedom—and the structure with standard Lagrangian elements.

Although the dynamic response of structures subjected to UNDEX loading has been extensively studied, most

coupled numerical approaches—such as CEL, ALE, BEM and CASA—still face significant limitations in terms of computational cost and efficiency. Full-scale simulations of complex structures exposed to near-field UNDEX often require several days on high-performance computing systems, due to the need for large computational domains, fine spatial resolution, and sophisticated algorithms to handle the interaction between fluid and structural domains [24, 38]. The complexity of managing mesh deformation, wave propagation, and phase coupling across different formulations contributes to this high demand. These challenges underscored in recent years the need for more efficient, accurate, and scalable numerical strategies capable of delivering real-time reliable predictions within reasonable computational timeframes across a wide range of engineering applications.

Integrating artificial intelligence (AI) and machine learning (ML) techniques into this framework represents a powerful and forward-looking approach to addressing this challenge [58]. These methods are capable of identifying complex, nonlinear relationships between input parameters and system responses by processing large datasets (from both experimental measurements and numerical simulations [59]) derived from intricate physical phenomena. Through a structured training process, AI and ML algorithms enable systems to learn from prior data and improve performance over time, without the need for explicit programming of the underlying physical rules [60, 61].

Data-driven approaches, supported by large datasets, have been successfully applied across various disciplines [60], including computer science [62], structural and fluid mechanics [63–65], air blast extreme events [66] and materials engineering [67].

Compared to traditional experimental, analytical and numerical methods, these novel techniques offer high precision, low computational cost, and the ability to efficiently address both forward and inverse problems. For instance, they can accurately predict material nonlinearities, structural deformations, as well as infer loading conditions from observed data and finally reconstruct FSI effects [67].

Especially in recent years, the inherent complexity of UNDEX scenarios—marked by strong nonlinearities, high strain-rate effects, and intricate FSI—has prompted a growing interest in alternative modeling strategies that can overcome the limitations of traditional numerical approaches. Researchers have increasingly explored the integration of ML and AI techniques into the simulation pipeline, aiming to reduce computational costs while maintaining a high level of accuracy and generalizability [24]. The way in which ML and AI have been incorporated across these stages—ranging from data generation to model training and evaluation—is schematically represented in Fig. 1, which outlines the conceptual framework underpinning this review.

Although the literature already includes several reviews on UNDEX, each addressing different aspects such as numerical modeling [3], the role of composite materials [1], the response of thin-walled metallic structures [68], fracture behaviour of plate specimens [69], measurement technology [70], UNDEX FSI [71] and ship damage and stability [72], there is currently no comprehensive study that explores in depth the potential of AI and ML in enhancing the prediction of UNDEX effects.

The primary goal of this article is to review recent advancements in the application of AI and ML techniques for predicting both the structural and fluid dynamic responses of systems subjected to UNDEX loads. By analyzing state-of-the-art methodologies, datasets, and modeling strategies, the article aims to highlight the strengths and limitations of current approaches, identify existing research gaps, and

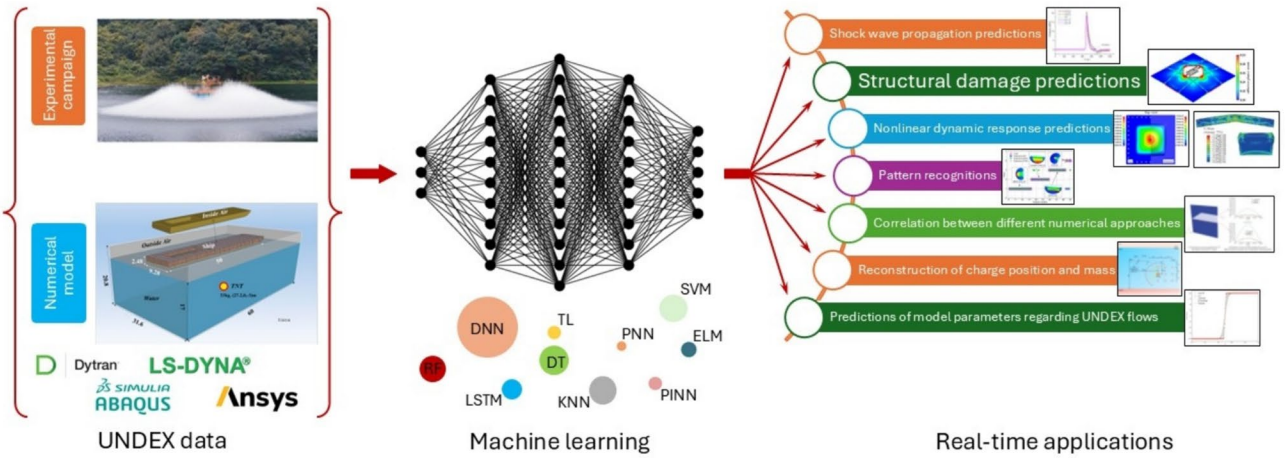

Fig. 1 General conceptual framework summarizing the key components, data flow, and methodological structure typically involved in ML approaches for UNDEX prediction

assess the suitability of various AI and ML architectures for different aspects of UNDEX analysis. In addition, based on the findings of this review, the article proposes a set of recommendations and guidelines to support the development of future research in this area.

The paper is organized into six main sections: the Introduction outlines the motivation and context of the study; Sect. 2 describes the methodology adopted for the literature review; Sect. 3 provides a concise overview of the physical phenomena associated with UNDEX events; Sect. 4 focuses on the numerical strategies most commonly used to generate datasets for ML applications in this context; Sect. 5 presents an in-depth analysis of the AI and ML techniques currently employed for UNDEX prediction tasks; finally, Sect. 6 discusses the main findings, identifies open challenges, and proposes future research directions for effectively integrating AI and ML into accurate and efficient UNDEX simulation frameworks. The structure of the paper is designed to provide the reader with a unified overview of all key aspects involved in the application of AI and ML to UNDEX predictions.

2 Literature Review Methodology

To identify relevant contributions for this study, a structured literature search was conducted using a combination of manual analysis and automatic processing of metadata, using both Scopus and Google Scholar as primary search databases, which are widely recognized as comprehensive academic databases encompassing most peer-reviewed articles indexed by the Web of Science. The search focused on retrieving studies related to the application of AI and ML in the prediction of UNDEX effects on structures. Keywords such as "underwater explosion", "machine learning", "deep learning", "shock response", "fluid–structure interaction", "damage prediction", "structural response", "numerical simulation", and "data-driven model" were used in various combinations with Boolean operators such as "AND" and "OR" to form effective search queries. The literature search covered publications up to the year 2025 (April 10, 2025). Nevertheless, given the recent and emerging nature of the topic, no relevant contributions were found before 2018, highlighting the novelty and growing interest in the new field. The search outcomes from Scopus and Google Scholar were then merged while eliminating the duplicate literature.

The article screening process has led to the inclusion of 23 papers in the study. Table 1 provides an overview of the bibliometric features of the 23 selected studies, including the publication timespan (up to April 2025), the number of unique sources (19), the average age of the articles (1.25 years), and the average number of citations per article (25.3). The relatively recent nature of this research domain is confirmed by the absence of contributions before 2018 and the observed average age. As expected, the most recent publications tend to receive fewer citations than earlier ones.

Table 1 Overview of the characterization of papers included in the studies for review

Feature	Quantification
Timespan	Over time until April 2025
Sources	19
Documents	23
Annual growth rate	29.17%
Authors	126
Authors of single-authored docs	0
International co-authorship	43.5%
Co-authors per doc	5.48
Author's keywords	182
References	1894
Document average age	1.25
Average citations per doc	25.3

Regarding the source of the papers included in this review, Elsevier Ltd, Springer Nature, and the Multidisciplinary Digital Publishing Institute (MDPI) account for most of the articles. Elsevier Ltd includes the following journals: "Ocean Engineering", "Journal of Computational Physics", "Defence Technology" and "Composite Structures"; Springer Nature includes journal such as "Journal of Marine Science and Application"; and finally, MDPI includes "Computation" and "Journal of Marine Science and Engineering". Figure 2 illustrates the distribution of the selected articles by year of publication. The trend reveals a clear increase in publication activity over time, particularly from 2022 onwards, although the growth is not strictly linear. While the earliest relevant contributions appeared in 2018 and remained sparse until 2021, a marked rise can be observed starting in 2022. The peak was reached in 2024 with 7 publications, followed closely by 6 in 2025; however, the number for 2025 is expected to increase, as the review covers publications only up to April 10, 2025. These numbers suggest a growing interest in the application of AI and ML techniques for UNDEX prediction, especially in the last four years. The increasing trend reinforces the recent and emerging nature of this research field and the motivation of this work.

Figure 3 presents the subject area distribution of the reviewed studies applying AI and ML techniques to UNDEX prediction problems. As expected, most of the works (82.61%) focus on naval structures or structural components with direct relevance to naval applications. This predominance reflects the critical importance of understanding and predicting the structural response of ships and submarines

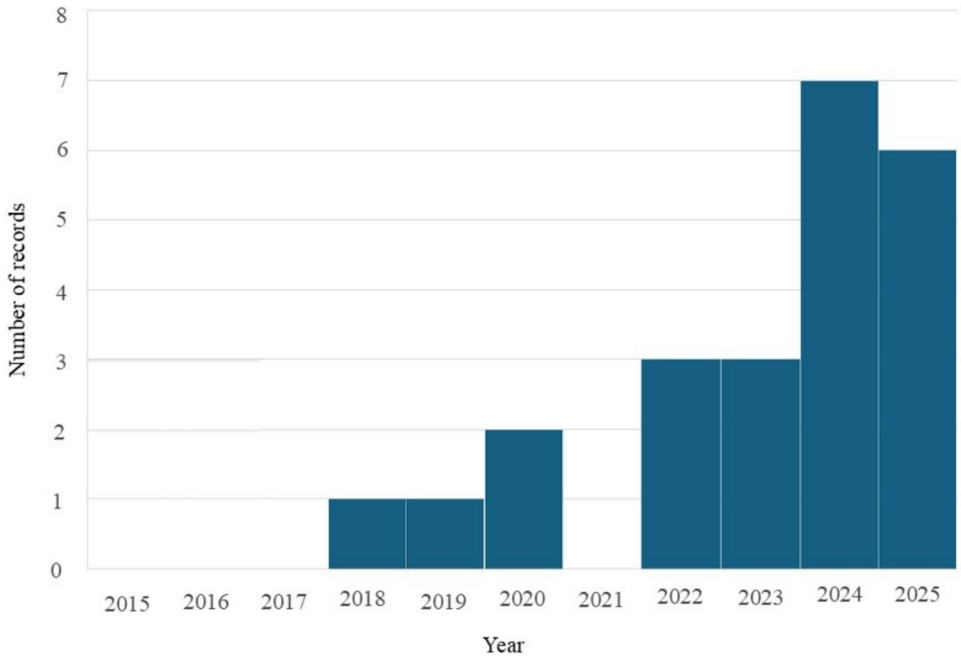

Fig. 2 Publication by year of the included studies. Records derived from the search conducted on April 10, 2025

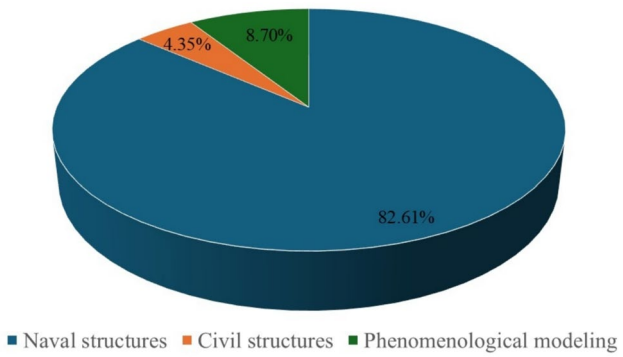

Fig. 3 Subject area flow chart for application of AI and ML to UNDEX predictions

to UNDEX loads, which is the primary concern in UNDEX-related research. A smaller contribution (8.70%) is dedicated to phenomenological modeling, in which AI and ML are employed to predict fluid-related parameters (e.g., pressure peaks, shock wave propagation, etc.) without direct reference to structural components. Finaly, a minor portion of studies (4.35%) extends the application of AI and ML methods to civil structures, such as dams, where blast mitigation remains relevant. This distribution highlights the dominant role of naval applications in the current research landscape, while also pointing to emerging interdisciplinary trends.

Figure 4 shows the global scientific production related to the reviewed studies. The map reflects the total number of publications in which at least one author is affiliated with a given country, regardless of their authorship role. China clearly dominates the research landscape, contributing to 18 of the 23 analyzed studies. The United States, Italy, United Kingdom and Cipro also appear on the map, each contributing a smaller number of publications. The intensity of the blue shading corresponds to the number of contributions, with darker shades indicating higher scientific output. The results emphasize that China is currently the most active country in this research domain, which aligns with its growing investment in AI and ML-based technologies and naval defense-related research.

Science mapping is presented in Fig. 5 (keyword co-occurrence map) and in Fig. 6 (word cloud). The keyword co-occurrence network shown in Fig. 5 was generated using the VOSviewer tool (version 1.6.20) and highlights the conceptual structure of the literature. Strong links are visible between central nodes such as “underwater explosion”, “machine learning”, and “dynamic response”, while peripheral clusters connect to more specific topics like “seabed detection”, “stiffened plate”, or “shock wave coupling effect”. The size of the nodes reflects the frequency of each keyword, and the link thickness indicates the strength of their co-occurrence.

The word cloud, generated using a Python-based script, displays the 50 most frequently used terms extracted from the selected papers (Fig. 6). As anticipated, core terms such as “machine learning”, “underwater explosion”, “structural response”, “deep neural network”, and “numerical simulation” appear with the highest frequency, reflecting the central focus of the reviewed studies. Other recurrent expressions include “blast load”, “damage estimation”, and “fluid–structure interaction”, which indicate

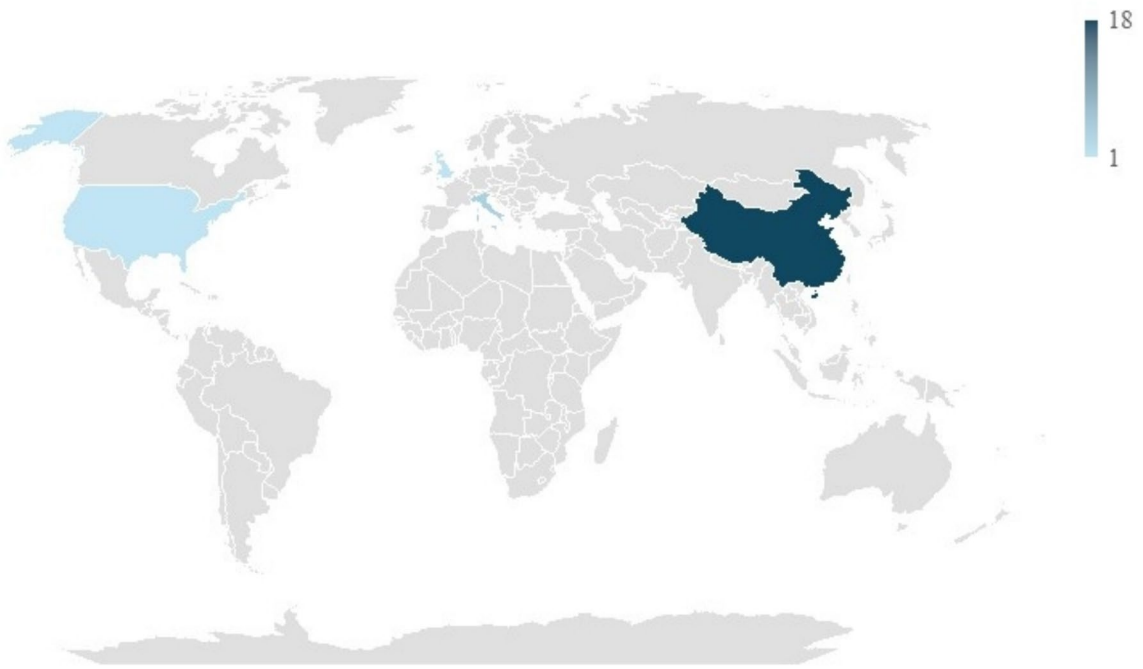

Fig. 4 Distribution of included studies per region in terms of article authorship: global map of the scientific production frequency

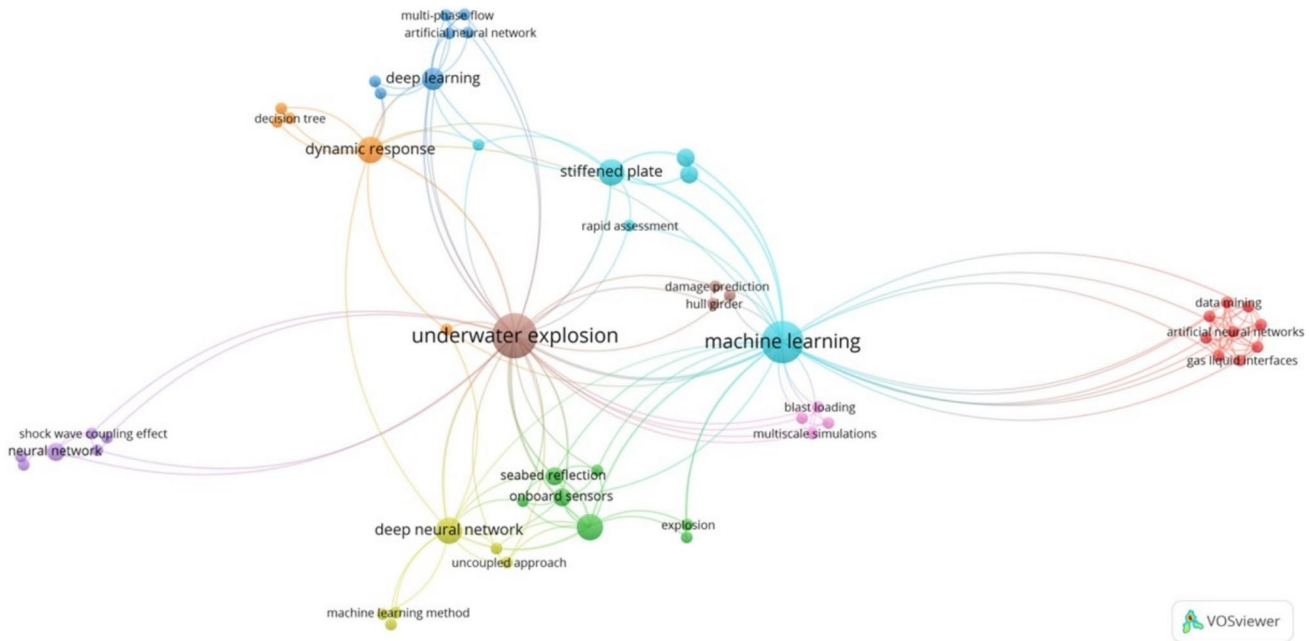

Fig. 5 Keywords co-occurrence

the multidimensional nature of UNDEX prediction, involving both structural and hydrodynamic aspects.

Together, these maps confirm that the application of AI and ML in the context of UNDEX modeling is a growing and multidomain field, with connections across structural dynamics, simulation, and data-driven aspects.

After outlining the main characteristics of the studies included in this literature review, the next section provides

Fig. 6 Word cloud visualization of the 50 most frequent terms within the included studies

a brief overview of the physical foundations of the UNDEX phenomenon. This section is intended to highlight the inherent complexity of UNDEX-related phenomena, which involve multiple interacting effects—such as shock wave propagation, cavitation, FSI, and structural damage mechanisms—that significantly challenge both modeling and especially accurate AI and ML predictions.

3 UNDEX Physical Reminder

The physical phenomena associated with UNDEX are inherently complex and highly nonlinear, involving extreme temperatures and pressures, transient multiphase states, large structural deformations, cavitation effects, and strong FSI [1, 24, 49, 73, 74]. A fundamental distinction between underwater and air explosions lies in the presence of the surrounding fluid medium, which results in the formation of a high-pressure, high-temperature gas bubble [69, 75, 76]. This bubble rapidly expands due to the energy released by detonation products, displacing the surrounding water and producing an outward-propagating shock wave.

As the bubble expands, its internal pressure decreases, while the ambient hydrostatic pressure begins to dominate, initiating a contraction phase. Due to the inertia of the surrounding fluid, the bubble contracts past its equilibrium radius before re-expanding—though less intensely—under residual internal pressure [72]. This results in a sequence of oscillations known as bubble pulsations, which gradually lose energy but can significantly impact submerged structures during each cycle [21, 77].

The structural loading induced by a typical UNDEX event can be broadly categorized into two main phases [1]: (1) an initial shockwave pressure spike resulting from the detonation, which is intense but brief, and (2) secondary loading effects generated by the pulsating motion of the bubble and associated jetting phenomena.

Figure 7 graphically represents the pressure trend during these two phases: an initial intense pressure surge from the impulsive shockwave, followed by oscillating pressure peaks caused by the pulsating bubble's ascent towards the surface.

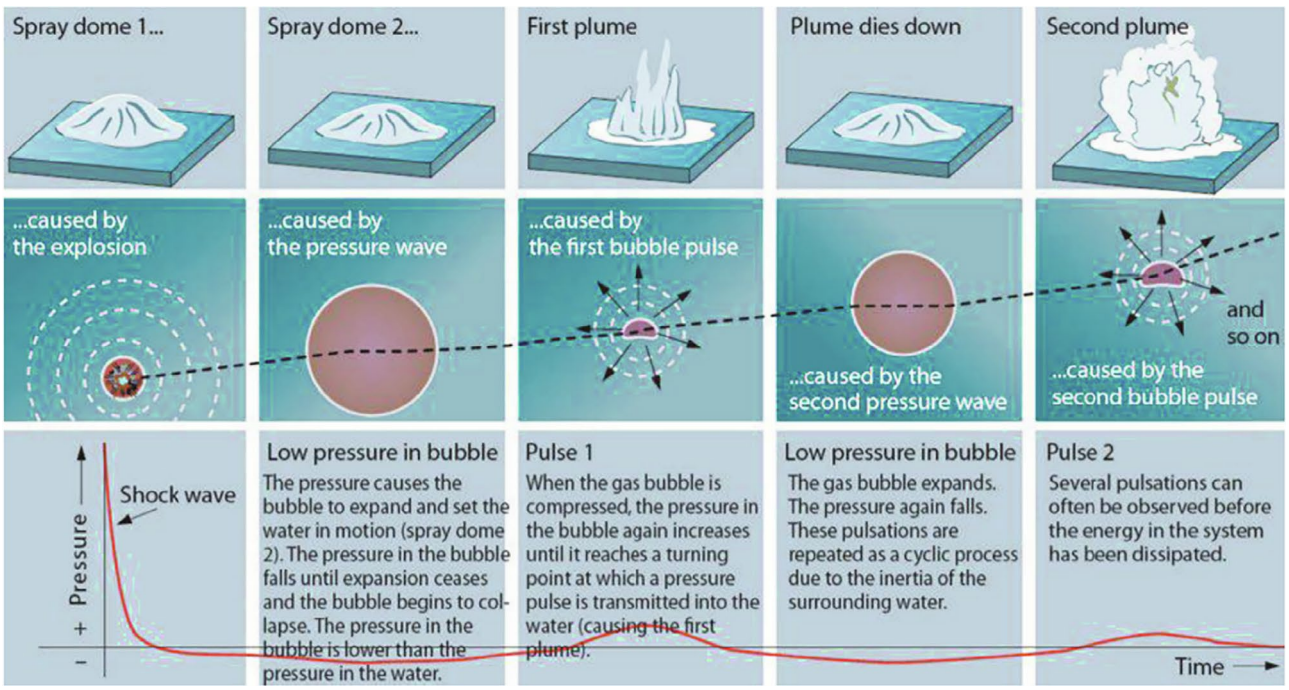

Fig. 7 Dynamics of the UNDEX event, capturing surface phenomena, bubble evolution, and pressure variations over time. Reprinted with permission from [1]

While the initial shock wave from the explosion is intense, impulsive, and brief, the pulsations from the gas bubble persist for a longer duration (fractions of a second), potentially causing fatigue damage to structures [78]. Furthermore, the oscillations of the gas bubble generate pulsating loads of lower magnitude and frequency compared to the primary shock wave. These oscillations can become hazardous if their frequency aligns with the natural frequencies of the hull beam, potentially leading to resonance and whipping motions, which are critical for ship hulls [50]. The pulse frequency, typically ranging from 1 to 3 Hz, is influenced by the explosive charge and the depth of detonation. This frequency range can cause resonance with the ship's first vertical bending modes [79, 80].

An added layer of complexity arises from the interaction between the shock wave, the free surface, and the seabed, depending on the specific scenario. During a typical UNDEX event, pressure monitored at a fixed point will detect not only the incident wave but also the reflected waves from both the seabed and the free surface [81–84]. The reflections of the shock wave from both the seabed and the free surface occur in such a manner that the angle of incidence is equal to the angle of reflection for both interfaces. This characteristic allows for the clear delineation of the various wave paths converging at the investigated point. Due to the differing paths, each wave will arrive at the point in succession rather than all at once, which leads to additional sequential loading on the structure. Although these reflected waves exert loads that are generally secondary compared to the primary direct loads from the explosion, they should not be overlooked, as their impact can still be significant in certain conditions [49]. In particular, the timing and interaction of these secondary loads can introduce complex stress patterns and may amplify the structural response, especially when the system is already under considerable strain. Therefore, while their intensity may be lower than that of the direct shock wave, these reflected waves contribute to the overall distribution and, depending on the specifics of the interaction, can play a non-negligible role in the structural response [85, 86].

In addition to the previously discussed phenomena, cavitation is another critical process that has been extensively investigated in the context of UNDEX [21, 87–89]. Cavitation in UNDEX events occurs due to rapid pressure fluctuations induced by shock and rarefaction waves, leading to the formation, growth, and subsequent collapse of vapor bubbles. This process profoundly affects pressure distribution, shock wave propagation, and the overall hydrodynamic behavior of the explosion. The collapse of cavitation bubbles generates additional shock waves and fluid motion, significantly altering the structural response. These induced shock waves and fluid flows not only exacerbate the loading on structures but also contribute to various damage mechanisms, potentially intensifying the destructive effects of the explosion. For instance, the implosion of these bubbles near structural surfaces can produce high velocity microjets and localized shock waves, leading to material erosion and fatigue over time. These interactions underscore the necessity of incorporating cavitation effects into numerical models to enhance the accuracy of UNDEX simulations.

This section has provided an overview of the primary and secondary effects associated with UNDEX, detailing complex physical processes such as shock waves, gas bubble pulsations, reflected waves, and cavitation. The intricate interplay of these phenomena renders the overall behavior of UNDEX highly complex and challenging to model. Consequently, recent advancements in research have seen a growing interest in applying AI and ML models to better understand and predict various aspects, particularly structural responses, to UNDEX events. These efforts reflect the increasing recognition of the need for more effective and efficient modeling tools to address the challenges posed by the dynamic and highly variable nature of UNDEX [37].

4 Dataset Generation Methods for AI and ML in UNDEX Application

AI and ML models require a substantial amount of data to be properly trained and to generate reliable predictions [59, 90]. This data can be obtained through experimental campaigns, which provide direct measurements of the phenomenon of interest, or generated via numerical simulations (common approach), offering a flexible and cost-effective alternative for exploring a wide range of scenarios (Fig. 1).

In research on AI and ML methods applied to UNDEX problems, the typical and common approach involves first developing a validated numerical model to capture the results of one or more experiments. Once the model has been verified against experimental data, a series of new numerical simulations is then conducted to generate a large dataset to be used for the training phase. This approach is necessary because the available literature offers a limited number of UNDEX experiments, which are rarely sufficient to ensure the proper training of ML algorithms. Numerical simulations, therefore, play a crucial role in expanding the dataset and improving the generalization capabilities of these models.

Since the topic addressed in this work is inherently multidisciplinary—spanning structural dynamics, fluid mechanics, and data science, this section aims to recall and synthesize the numerical strategies most used in the literature to generate datasets for AI and ML applications in UNDEX scenarios. While various numerical approaches exist for simulating underwater explosions [3], this section focuses specifically on those that have been effectively used to produce training data for data-driven predictive models. Other numerical methods,

although not detailed here, have been already referenced in the introductory section of this work.

4.1 Finite Element Method (FEM)

The simplest approach for simulating UNDEX events—especially for the purpose of generating datasets for AI and ML models—is to use the traditional purely Lagrangian finite element method (FEM) [2]. This strategy consists of applying a time-dependent pressure history, obtained from analytical expressions or experimental data, directly onto the structural model of the target (wetted surface, Fig. 8). However, this method neglects FSI effects, which can significantly influence the structural response. Due to these limitations, this approach is rarely used in advanced UNDEX analyses, despite being one of the earliest approaches in historical UNDEX analyses.

4.2 Coupled Eulerian–Lagrangian (CEL) and Arbitrary Lagrangian- Eulerian (ALE)

The CEL method integrates Eulerian and Lagrangian mesh formulations within a unified simulation framework to effectively model FSI, especially under extreme loading conditions such as UNDEX. The Eulerian formulation is particularly suited for representing fluids—including explosive products, water, and air—as it uses a mesh that remains fixed in space while material flows through it. This is achieved through advection algorithms that track the movement of physical quantities across the mesh [91, 92]. Conversely, the Lagrangian formulation is employed for modeling solid bodies, where the mesh moves with the material. This makes it highly effective in capturing structural deformation and stress wave propagation [93].

In CEL simulations, the Eulerian regions are typically assigned to materials like the explosive charge, the surrounding water, and air pockets, each requiring an appropriate equation of state (EOS) to capture its thermodynamic behavior. For instance, the explosive is often modeled using the Jones–Wilkins–Lee (JWL) EOS, which characterizes the detonation products in terms of pressure–volume–energy relationships [94]. The surrounding water may be modeled with a Mie-Grüneisen [47] or polynomial EOS [95], while air—if explicitly modeled—is usually represented by the ideal gas law [25]. These EOS models are critical in capturing shock wave transmission and interactions across different media. These regions are generally solved using the finite volume method (FVM), which is well-suited for handling compressible flows and shock wave propagation.

The structural components, such as the target structure or seabed, are modeled using a Lagrangian formulation (e.g. FEM), which follows the motion of the material and mesh together. To accurately predict their mechanical response, each Lagrangian region must be assigned a suitable constitutive model that accounts for plasticity, damage, or other nonlinear behavior under high strain rates [96].

To facilitate load transfer and mutual interaction between fluid and solid domains, a specialized coupling algorithm is implemented [96]. This allows for the real-time exchange of forces and displacements across the fluid–structure interface (e.g. coupling surface), effectively resolving the complex dynamics of FSI [41]. Phenomena such as cavitation, reflection, gas bubble pulsation and transmission of shock waves are inherently captured, enhancing the fidelity of the simulation [12, 21]. To summarize, a 2D schematic of the CEL approach is presented in Fig. 9.

The ALE method shares many conceptual similarities with CEL but offers enhanced capabilities for handling large deformations. The primary advantage of ALE lies in its mesh rezoning or remeshing capability, where the computational mesh can be dynamically updated or adapted during the simulation [9, 97–99]. This helps reduce numerical instabilities and mesh distortion, which are common in purely Lagrangian formulations when elements undergo extreme deformation or collapse. In ALE, the mesh motion can be decoupled from material motion, allowing it to either follow the flow or maintain element quality in critical regions.

This distinction between CEL and ALE is well illustrated in Fig. 10. In the initial configuration, the fluid domain (light blue) is discretized using Eulerian elements with a fixed grid, while the structural domain (outlined in red) is modeled using a Lagrangian mesh. In the CEL final configuration, the fluid moves through the fixed Eulerian mesh, and the structure deforms with its mesh. In contrast, the ALE final configuration shows the mesh adapting dynamically (rezoned mesh) to better follow the flow of the fluid and improve element quality, which enhances numerical accuracy and reduces artifacts caused by severe mesh distortion. Some simulation software platforms that implement CEL and ALE techniques also offer the option of an adaptive Eulerian mesh. In this approach, although the mesh remains fundamentally Eulerian, it is allowed to move or deform locally in response to the motion of the structure.

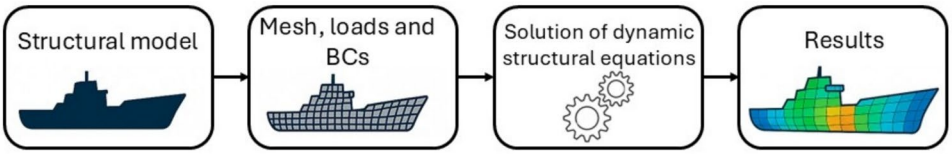

Fig. 8 FEM analysis scheme applied to a naval ship

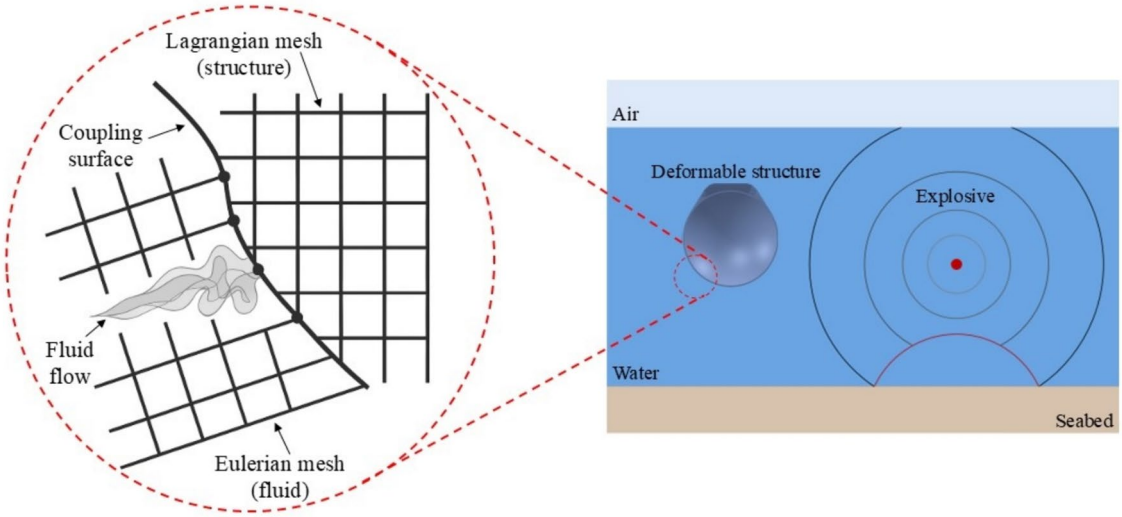

Fig. 9 CEL analysis scheme applied to the section of a submarine considering the detonation of the explosive, the wave propagation and FSI for a generic scenario

Despite their accuracy and robustness, both CEL and ALE approaches are computationally expensive, particularly for full-scale structural models or long-duration simulations. As several authors have noted [3, 24], the high cost in terms of memory and computational time limits their applicability to simplified geometries or localized models. To mitigate these costs, remapping techniques can be used to reassign solution variables between meshes, improving computational efficiency while preserving physical fidelity [100].

Based on the present review of the literature, CEL and ALE remain the most widely adopted approaches for generating high-fidelity datasets to train AI and ML models in UNDEX applications. Their ability to capture the complex physics of shock propagation and FSI with high resolution makes them particularly valuable in developing reliable data-driven predictive frameworks in UNDEX problems.

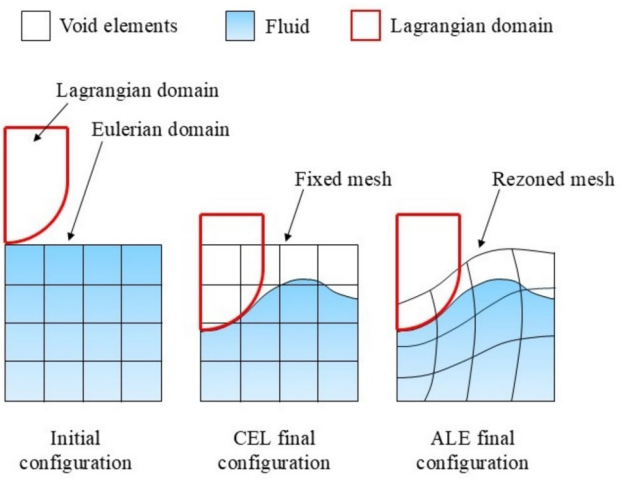

Fig. 10 Comparison of mesh motion between the CEL and ALE approaches

While both CEL and ALE approaches offer high-fidelity modeling of fluid–structure interaction in UNDEX scenarios, they also present specific limitations. The CEL method, although robust in capturing strong shock waves and cavitation phenomena, often suffers from high computational costs due to the need for fine Eulerian mesh resolution, especially in three-dimensional configurations. Additionally, managing material advection across the fixed Eulerian grid can introduce numerical diffusion, which may affect accuracy in tracking interfaces or small-scale features.

Similarly, the ALE method, despite its enhanced ability to handle large deformations through mesh rezoning, requires careful control of mesh motion algorithms and remeshing strategies to maintain numerical stability. The setup is generally more complex and sensitive to parameter selection, such as viscosity terms and mesh relaxation settings. Both methods also demand significant computational resources and are therefore not ideal for scenarios requiring rapid simulations or large-scale dataset generation for ML applications. These limitations should be carefully weighed when selecting the most suitable simulation strategy, depending on the specific goals of the study.

Finally, it is worth noting that in high-fidelity FSI simulations, the choice of numerical parameters—such as penalty factors or contact stiffness—can strongly affect local pressure distributions and structural loading. Based on the authors' experience, a consistent calibration of such parameters across simulations is recommended to ensure dataset homogeneity, especially when the numerical results are used

to train ML models. Parameter sensitivity analyses should be conducted during preliminary stages, and extreme values should be avoided to minimize artificial numerical artifacts.

4.3 Uncoupled Eulerian–Lagrangian (UEL)

The UEL approach adopts a two-step simulation strategy to analyze UNDEX effects on structures (Fig. 11). The first step involves computing the pressure field generated by the explosion, while treating the target structure as rigid. The second step assesses the structural dynamic response under the previously calculated pressure loading, ignoring FSI effects [24, 101]. In the first phase, the propagation of the blast wave through the surrounding fluid medium (typically water and air for UNDEX cases) is simulated using an Eulerian mesh formulation, solved using FVM. This step focuses on capturing the spatial and temporal distribution of pressure on the structure's surface, relying on the same EOS commonly employed in CEL and ALE methods.

Once the pressure–time history has been obtained, it is mapped onto the surface of the structure and used as an external load in a subsequent purely Lagrangian analysis. In this second phase, the structure is modeled as fully deformable, and its mechanical response is evaluated using appropriate constitutive models.

This uncoupled strategy allows a significant reduction in computational cost, primarily because it avoids the need to resolve the full fluid–structure interaction (FSI) in a coupled framework. The absence of FSI contact algorithms—normally required to capture mutual pressure feedback and interface behavior—greatly simplifies the numerical treatment and reduces solver time.

When dealing with submerged or floating structures, a key challenge in UEL simulations is the treatment of the added mass effect—the inertia of the surrounding fluid that moves with the structure. Unlike in CEL or ALE methods, where the fluid domain is explicitly included and naturally contributes to the system's dynamics, the UEL approach requires that added mass effects be accounted for manually in the structural model. This is particularly important in the second step, where the structure is isolated from the fluid and subjected to the pressure loading derived from the first step. If not properly considered, neglecting added mass can lead to significant underestimation of structural response [102]. For a detailed discussion and comparison of these implementation strategies in practical applications, the reader is referred to [102].

To illustrate the overall UEL procedure, Fig. 11 presents a schematic representation of its two main stages. In practical applications, additional sub-steps—such as pressure remapping or mesh adaptation—may be incorporated to improve computational performance and result fidelity.

As highlighted in [24], although the UEL approach is significantly more efficient from a computational standpoint than the fully coupled CEL and ALE methods, it suffers from a major limitation: the lack of direct FSI modeling. Therefore, results obtained through this strategy must be interpreted with caution. When high-fidelity results are required, post-processing corrections or hybrid methods may be necessary to approximate the influence of neglected FSI effects. For this reason, very few studies in the literature rely on UEL-based simulations to generate training datasets for AI and ML models in UNDEX applications, as the lack of coupled physics may compromise the generalization and reliability of the predictive models trained on such data.

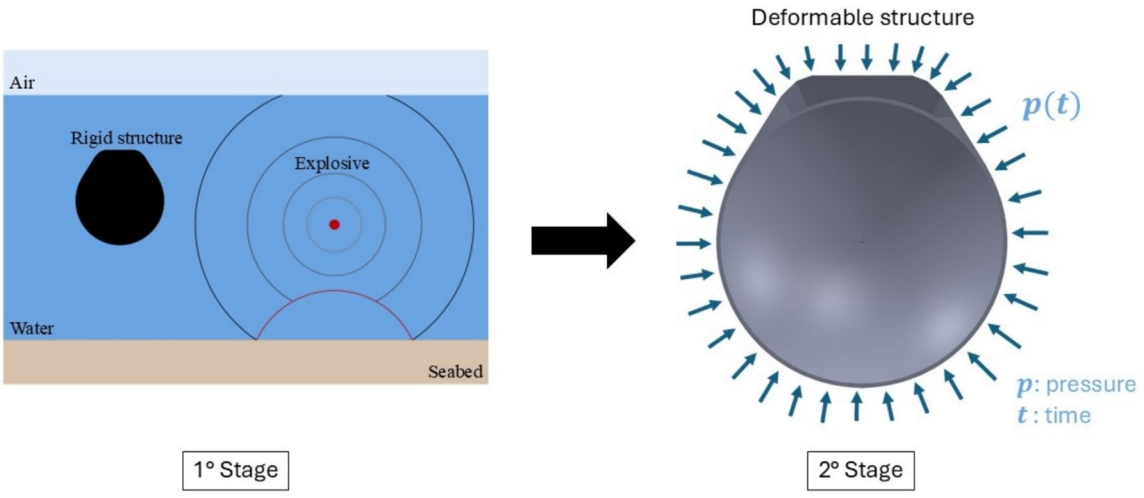

Fig. 11 UEL scheme applied to the same structure of Fig. 9: an Eulerian simulation considers detonation of the explosive and wave propagation. The pressure is mapped and consequently applied to the structure in a Lagrangian simulation

4.4 Coupled Acoustic-Structural Approach (CASA)

The core of the CASA numerical approach is to divide the UNDEX impact process into two stages: the first, involving the propagation of the shock wave through the fluid medium before reaching the structure, and the second, concerning the interaction between the incident wave and the structure itself. The simulation focuses exclusively on the second stage, intentionally neglecting the detailed modeling of the incident wave's travel through the water. Within this framework, water is represented using acoustic elements that solve the linearized acoustic wave equation, while the structure is modeled using a standard Lagrangian FEM [1]. This allows for efficient FSI through a coupling surface—typically the wetted area of the structure—without requiring a full Eulerian treatment of the surrounding fluid.

To apply pressure loading resulting from the incident wave, an acoustic-field initialization is introduced at the start of the numerical analysis [33, 56]. This involves defining a spatially distributed pressure field within the acoustic domain, typically based on the expected time history of the shock wave. In this context, a source point is a theoretical location representing the origin of the explosion, while a reference point (called also standoff point) is a user-defined point in the acoustic domain, located at a known distance from the source, where the pressure–time history is specified (see Fig. 12). The reference point serves as a proxy for calibrating the temporal characteristics of the shock wave, such as peak pressure, duration, and decay rate [103].

Since high-fidelity pressure–time histories measured by experiments are rarely available, empirical formulations are commonly used to estimate the peak pressure and decay profile of the shock wave [21, 104]. These empirical relations allow the user to define a pulse history at the reference point. Using the known spatial relationship between the source and reference points, the software interpolates or propagates this pressure field throughout the acoustic domain. This enables the representation of the wave's arrival and loading on the structure surface without explicitly simulating the wave's full propagation from source to target.

This approach is implemented in several commercial finite element codes, including LS-DYNA and ABAQUS/Explicit [57], which provide specialized features for defining acoustic domains, fluid–structure interfaces, and non-reflecting boundaries to simulate semi-infinite fluid media. Although this strategy significantly reduces computational cost and complexity, it also introduces approximations, especially in scenarios where complex wave reflections, cavitation, or bubble effects are significant. Nonetheless, for many practical engineering applications, the CASA approach remains a valuable and pragmatic solution for assessing the structural response to UNDEX events. This method is well-known in UNDEX literature, but it has been used only sparingly in AI and ML applications. An example of the application of the CASA approach to a full-scale vessel is presented in Fig. 13.

4.5 Boundary Element Method (BEM)

The Boundary Element Method (BEM), also known as the Boundary Integral Method (BIM), is a numerical technique used to solve linear and nonlinear partial differential equations (PDEs) by reformulating them as boundary integral equations. Unlike traditional domain-based methods such as

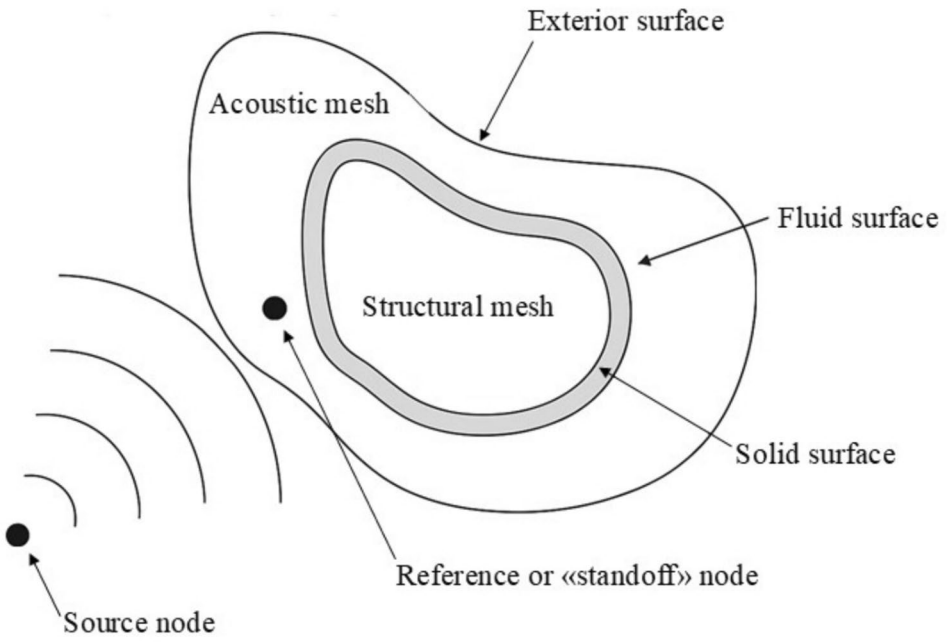

Fig. 12 General scheme of the CASA approach

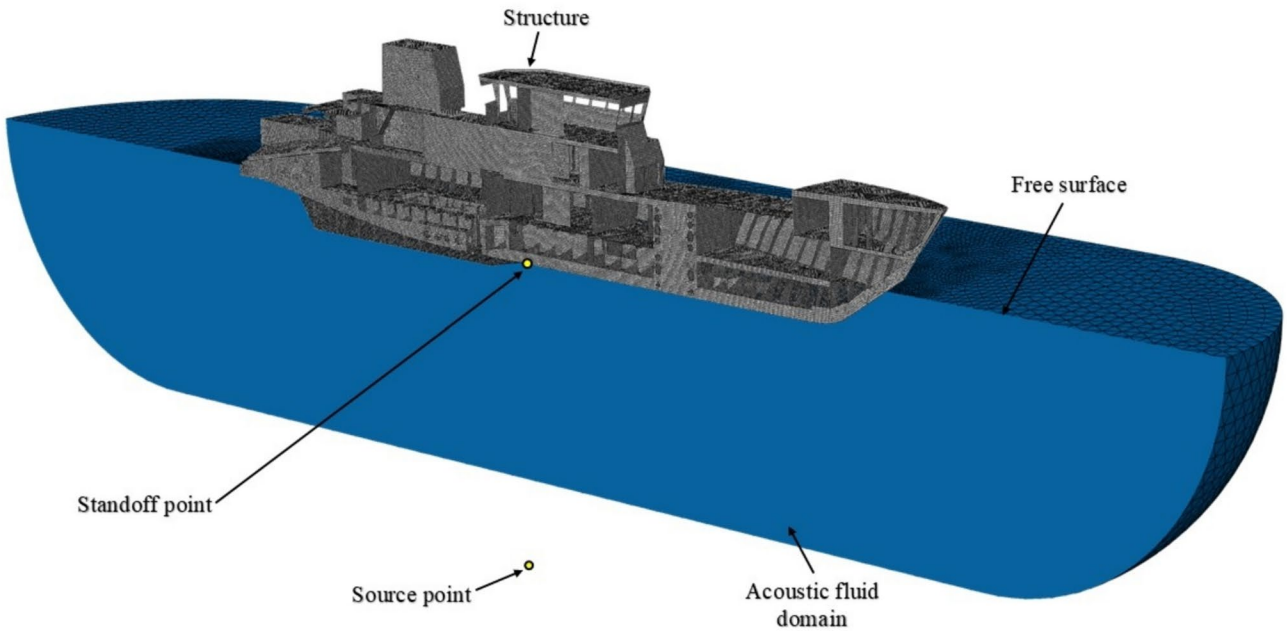

Fig. 13 Example of a CASA numerical model involving a generic ship structure. Vertical cut of the model to better understand the features of the scenario

the traditional FEM and CEL/ALE, which require discretization of the entire domain, BEM requires discretization only along the boundaries of the problem domain. This reduction in dimensionality—from volume to surface in 3D problems, or from area to line in 2D problems—leads to a significant decrease in computational effort, particularly advantageous in large-scale or unbounded problems [105, 106].

The foundations of BEM are rooted in Green's functions and potential theory, which allow the solution inside the domain to be expressed in terms of values on its boundary. This makes BEM especially attractive for problems involving infinite or semi-infinite domains, such as acoustic scattering, electrostatics, elasticity, and fluid flow [3]. Since BEM naturally satisfies far-field boundary conditions without the need for artificial truncation, it eliminates a major source of error common to volume-discretization methods.

One of BEM's most significant advantages is its high accuracy near boundaries, where the most critical interactions typically occur in physical systems. The method is well-suited for handling complex geometries, moving interfaces, and singularities. In FSI and UNDEX problems, BEM has gained considerable attention due to its ability to accurately simulate transient free surface flows and moving boundary conditions, such as those encountered during bubble collapse or cavitation. The method's inherent formulation makes it especially powerful for tracking the time-dependent evolution of bubble geometry, pressure distribution, and interactions with nearby structures. An example of the application of the BEM to study the interaction between a three-dimensional bubble and the free surface is presented in [106], with a visual depiction provided in Fig. 14.

5 Artificial Intelligence and Machine Learning Techniques for UNDEX Predictions

5.1 Introduction

In recent years, AI has emerged as a transformative force with far-reaching impact across numerous domains. Its broad spectrum of applications highlights its potential to revolutionize how problems are approached and solved. The term AI was first introduced by John McCarthy in 1955 [107] and refers to the branch of computer science that enables machines to replicate human cognitive functions such as learning, reasoning, and self-correction [108]. AI systems are designed to handle complex tasks in ways that resemble human problem-solving, drawing on diverse methodologies including ML, deep learning (DL), and rule-based systems.

ML is a branch of AI that allows computer systems to learn and improve their performance through experience, without the need for explicit programming [109]. It involves algorithms that can detect patterns in data and make predictions or decisions based on that data. As the algorithms are exposed to more training data, their performance typically improves [110]. Effective issue solving depends on selecting the appropriate data and organizing it correctly [111]. To

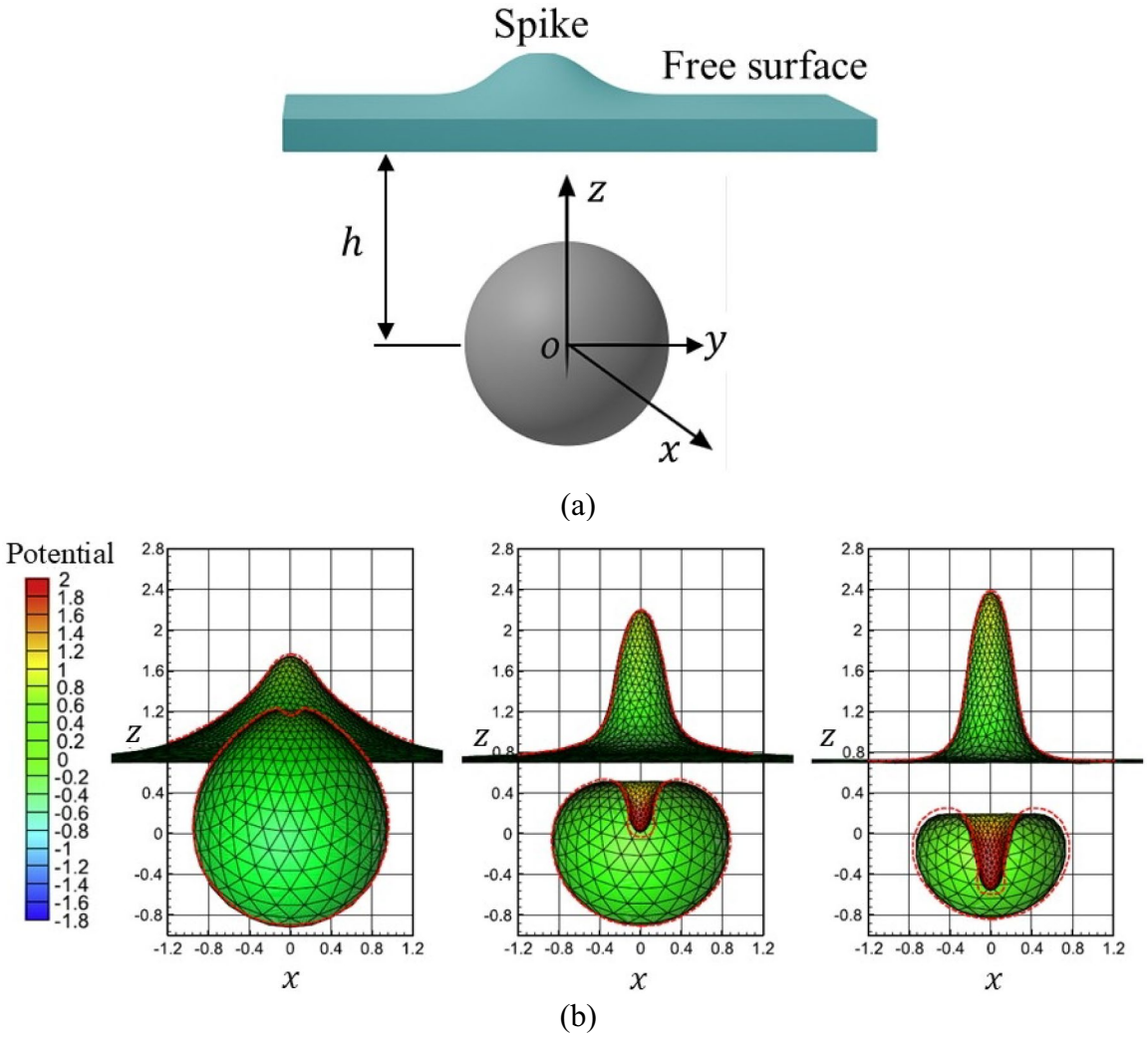

Fig. 14 **a** Scheme of the scenario and **b** evolution of the bubble near free surface at different time instants with an indication of the potential (energy per unit volume). Adapted from [106]

avoid repeated references to both AI and ML, the term ML methods will be used throughout the remainder of this work.

ML algorithms are generally categorized into four main types [112] (Fig. 15): supervised, unsupervised, semi-supervised and reinforcement learning (RL).

Supervised learning involves training models on labeled data to make predictions on new, unseen data, and it is the most used approach for UNDEX tasks such as classification and regression, particularly in UNDEX effects' predictions. Unsupervised learning, on the other hand, detects patterns and structures in data without the use of predefined labels. Semi-supervised learning bridges the gap between the two, combining a small amount of labeled data with a larger pool of unlabeled data during training. RL is a distinct paradigm in which an agent interacts with a dynamic environment, learning through trial and error to optimize its performance [113]. Since unsupervised, semi-supervised, and RL approaches are not yet employed in the context of UNDEX-related predictions, the following section focuses exclusively on supervised learning techniques and their applications in this field.

To effectively apply these supervised learning techniques to the prediction of UNDEX event features, a structured approach to data handling and model training is required (Fig. 16).

In the context of ML-based prediction of UNDEX event's features, raw experimental or simulated data (in the latter case, generated using the numerical methods presented in Sect. 4) are typically partitioned into three distinct sets: training, validation, and testing datasets. The training dataset is used to teach the ML model by allowing it to learn underlying patterns and relationships within the data. The validation dataset serves to monitor the model's performance during training and to identify signs of overfitting—an issue that

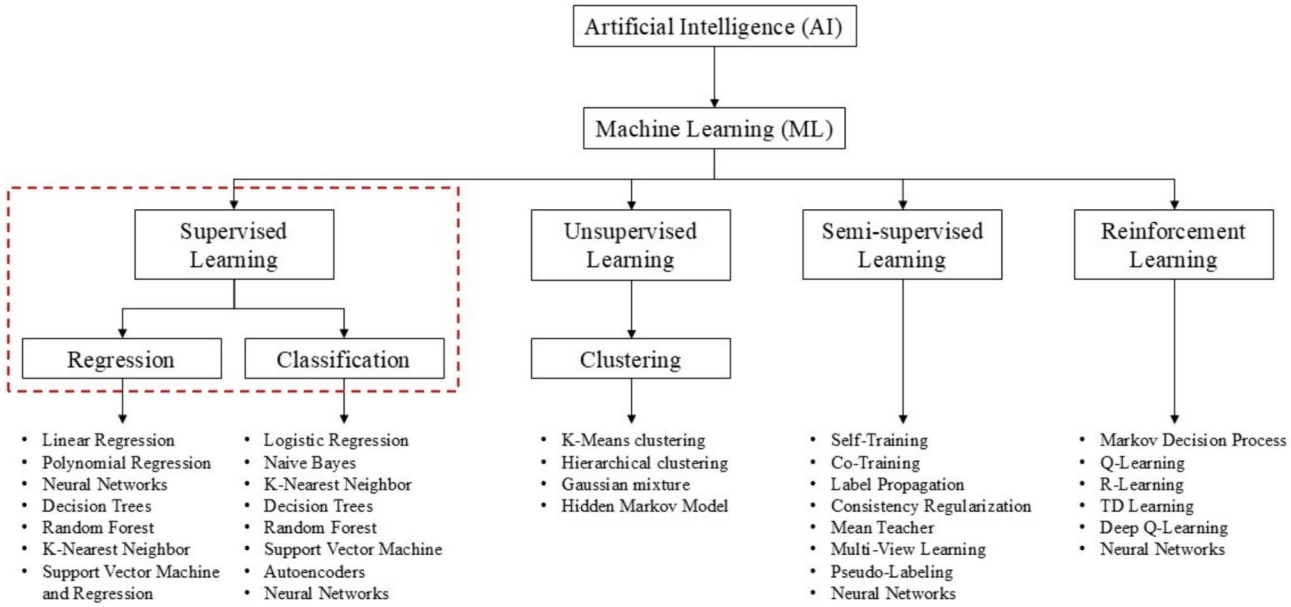

Fig. 15 General classification of AI and ML algorithms, with highlight of those employed for UNDEX prediction's tasks

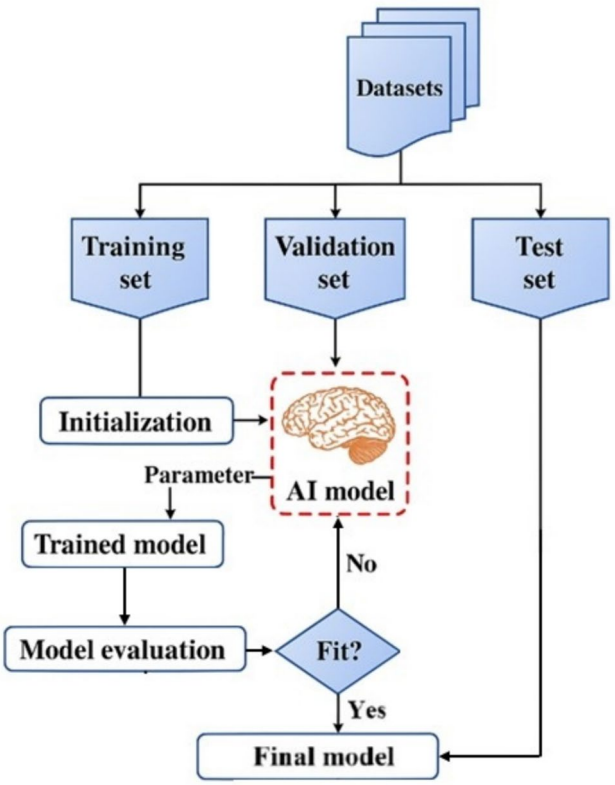

Fig. 16 Typical prediction process of ML-based method for UNDEX predictions

arises when the model becomes too tailored to the training data and performs poorly on new data [58]. By evaluating performance on the validation set, adjustments can be made to fine-tune the model's hyperparameters (the parameters that control the learning process and affect the model's performance) [114]. Once the model is trained and optimized, its predictive capabilities are evaluated using the testing dataset, which consists of previously unseen data. This final step provides insight into the model's generalization ability and its expected performance in real-world and real-time scenarios. The typical workflow of ML-based prediction for UNDEX event's effects is illustrated in Fig. 16.

5.2 Supervised Learning

Supervised ML, which relies on labeled datasets to train algorithms capable of making accurate predictions on new, unseen data, has emerged as a cornerstone technique in many engineering applications [115]. In supervised learning, the training process is guided by the input–output relationships explicitly provided in the dataset, allowing the model to learn the mapping between features and target variables. One of the key aspects in evaluating the performance and reliability of a trained model is the prediction error, which involves testing the model using new input data that was not included during the initial training phase. This step helps verify the model's ability to generalize and make reliable predictions outside the training environment [66].

Regression and classification represent the two principal subtypes of supervised learning, distinguished primarily

by the nature of the output variable they aim to predict. In regression problems, the target variable is continuous and can assume an infinite range of numerical values [25]. This makes regression models particularly suitable for estimating structural quantities such as displacement, FSI responses, plastic strain, and other relevant continuous metrics often encountered in UNDEX studies. These models allow researchers to quantify physical responses across a spectrum of loading conditions or material configurations, providing valuable insights for structural integrity assessment. Various regression models can be used for such predictions. However, many cases leverage the capabilities of Artificial and Deep Neural Networks, often employing multiple them in series to improve accuracy and robustness in the predictions.

In contrast, classification-based ML focuses on predicting discrete output labels, typically assigning input data to one of several predefined categories [111]. This approach is useful when the problem involves identifying the presence or absence of a condition (e.g., damage localization), categorizing types of failure modes, or detecting binary or multi-class states in structural health monitoring (SHM) scenarios. Classification tasks are essentially found in decision-support systems, where understanding the qualitative state of a structure, rather than its precise numerical response, is the priority. Despite their widespread application in other engineering domains, classification-based ML models have seen relatively limited use in the context of UNDEX studies, where the focus has traditionally been on predicting continuous physical quantities rather than categorical outcomes.

Despite the broad application of regression techniques in numerous UNDEX-related ML studies, there is still no universally accepted, coherent, or standardized metric for evaluating the effectiveness of regression outcomes [112]. As a result, a variety of performance metrics are commonly employed to assess model accuracy and reliability. Among the most widely used are: the mean square error $MSE = \frac{1}{m} \cdot \sum_{i=1}^{m} \left(X_i - Y_i\right)^2$, the mean relative error $MRE = \frac{1}{m} \cdot \sum_{i=1}^{m} \left|\frac{X_i - Y_i}{Y_i}\right|$, the root mean square error $RMSE = \sqrt{\frac{1}{m} \cdot \sum_{i=1}^{m} \left(X_i - Y_i\right)^2}$, the mean absolute error $MAE = \frac{1}{m} \cdot \sum_{i=1}^{m} \left|X_i - Y_i\right|$ and the coefficient of determination $R^2 = 1 - \frac{\sum_{i=1}^{m} \left(X_i - Y_i\right)^2}{\sum_{i=1}^{m} \left(\overline{Y} - Y_i\right)^2}$, where m is the number of predictions, X_i is the predicted i-th value and finally Y_i is the actual or target ith value.

For classification tasks, performance is typically evaluated using metrics that quantify the correctness of class assignments. The most common include accuracy (calculated by dividing the number of correct predictions by the total number of predictions), precision (proportion of true positives out of all positive predictions), recall (proportion of true positives out of all actual positives), F1-score (harmonic mean of precision and recall, providing a balance between the two) and confusion matrix, which provides a detailed breakdown of true positives, false positives, true negatives, and false negatives (showing how many instances were correctly or incorrectly classified in each category) [116]. These classification metrics are essential for understanding the model's behavior in distinguishing between discrete categories, and they offer complementary insights to those provided by regression-based evaluation tools.

While no universally accepted threshold values exist, several studies in related engineering applications suggest indicative target ranges. For instance, a coefficient of determination R^2 above 0.9 is often considered a strong fit in regression problems involving structural response prediction. *RMSE* and *MAE* are typically normalized with respect to the range of the target variable, and normalized errors below 10% are commonly used as a benchmark for satisfactory accuracy. *MRE* can vary widely depending on the scale of the outputs, but values below 0.1–0.15 are generally acceptable. *MSE* values are more difficult to interpret directly due to their unit dependence, but are useful for comparative purposes across models trained on the same dataset.

For classification tasks, performance is commonly considered acceptable when accuracy exceeds 85–90%, although more robust insight is often provided by F1-scores above 0.8, particularly in cases with class imbalance. These reference values, however, should always be interpreted in light of the specific prediction target, the variability and quality of the dataset, and the scale of the input/output quantities.

The following paragraphs provide a focused overview of supervised ML approaches applied to UNDEX-related problems, with a particular emphasis on both regression and classification tasks. Specifically, it is presented and briefly described the main categories of methods found in the literature, including: (i) Neural Network (NN)-based models, (ii) decision trees and tree-based ensemble methods, (iii) instance-based and distance-based learning algorithms, and (iv) advanced learning strategies.

5.2.1 Neural Networks (NN)-Based Models

Neural Networks (NN)-based models represent one of the most widely used and versatile classes of supervised learning ML models in the field of engineering and physical sciences [115]. They have become particularly popular in recent years for modeling and predicting the structural and fluid-dynamic effects associated with UNDEX, due to their ability to approximate highly nonlinear relationships between input parameters and system responses [29]. This section provides an overview of the main NN architecture

employed in UNDEX-related studies, discussing their underlying principles, structural differences, and specific applications within the context of underwater blast response predictions.

5.2.1.1 Artificial Neural Networks (ANNs) and Deep Neural Networks (DNNs) Artificial Neural Networks (ANNs) are foundational ML models inspired by the structure and functioning of the human brain. They consist of interconnected layers of processing units called neurons, which are organized into an input layer, one or more hidden layers, and an output layer [113]. Each neuron applies a transformation (usually nonlinear) to the incoming signals and passes the result forward through the network. ANNs are particularly effective in capturing nonlinear relationships between input features and target outputs, making them suitable for complex pattern recognition and regression UNDEX-related tasks. Historically, ANNs have been widely applied across various domains, including material science, hydrology, and engineering, due to their flexibility and relatively simple structure [39]. However, the effectiveness of ANNs is often limited by their shallow architecture—typically one or two hidden layers—which can restrict their ability to model more complex and hierarchical data representations.

To address this, Deep Neural Networks (DNNs) have emerged as a powerful extension of traditional ANNs. DNNs are characterized by having multiple hidden layers, allowing them to learn progressively abstract and high-level representations of the data (Fig. 17). DNNs can handle more intricate patterns, especially when working with high-dimensional or unstructured inputs such as images, time-series, or signals.

A key advantage of DNNs is their ability to automatically extract features from raw data, reducing the need for manual feature engineering [117]. However, this comes at the cost of increased computational demands, potential overfitting, and the need for large, labeled datasets and tuned hyperparameters to achieve optimal performance.

In the following, the main studies conducted so far in the UNDEX domain that have employed ANNs or DNNs for predictive modeling are summarized.

Bardiani et al. [24], employed a DNN to predict the displacement field of vertical submerged plates subjected to contact UNDEX loads, using features extracted from UEL and CEL simulations—such as out-of-plane displacement, equivalent plastic strain, mass-per-unit area, and explosion type. The model was trained on a dataset comprising paired coupled and uncoupled simulations, with data augmentation techniques applied to increase training robustness. The performance of the DNN was assessed through standard training/validation/test splits, with early stopping used to prevent overfitting. Results showed high predictive accuracy, with the DNN successfully learning to replicate the effect of FSI without the need for computationally expensive coupled analyses (like CEL or ALE). The model achieved a *MSE* of 0.002 on the test data, indicating its effectiveness in predicting the displacement field.

Shifting the focus, the work presented in [25] proposed a data-driven framework based on a DNN to classify the detonation point of contact UNDEX by leveraging pressure and displacement histories acquired at the central point on unstiffened plate structures. The DNN was trained using a comprehensive dataset of CEL simulations that incorporated various seabed types, material properties, and UNDEX geometrical configurations. Input features included seabed stiffness, structural properties, and key pressure/displacement metrics, while the output was a class corresponding to the

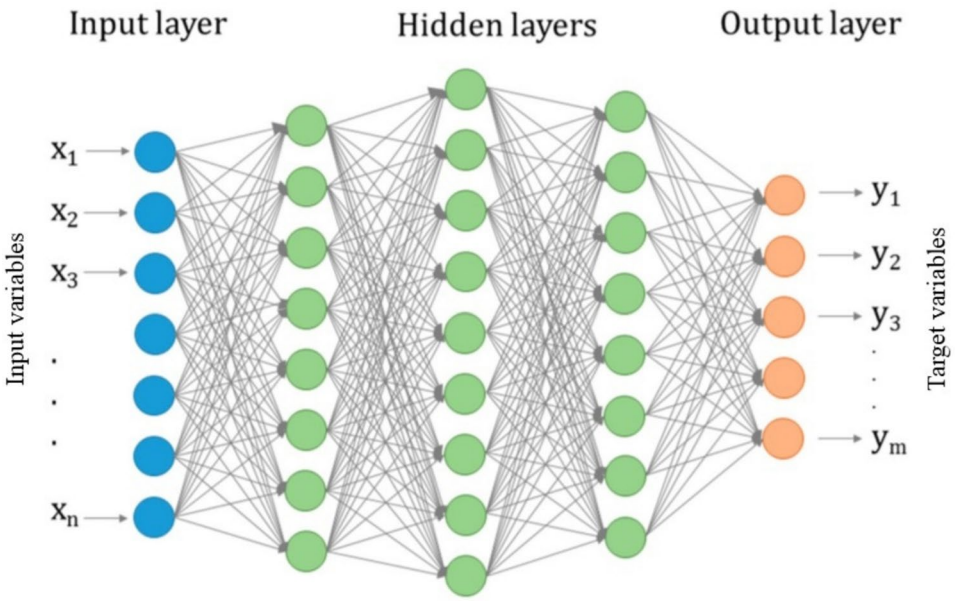

Fig. 17 General scheme of a Deep Neural Network (DNN) model. Adapted from [111]

explosive's location on a user-defined 2D grid. The method achieved high accuracy (F1-score of 99.16%) and is notable for being among the few examples applying ML to reconstruct actionable features from UNDEX events, with a clear emphasis on real-time applicability through sensor-based onboard measurements.

Building on this work, the same authors further explored the capabilities of their DNN model by applying it to a regression task aimed at predicting the mass of the explosive charge in UNDEX scenarios [29]. In this follow-up study, the authors utilized data from CEL simulations and notably introduced transfer learning for the first time in UNDEX context (see the paragraph specifically addressing this). Based on an extended dataset of 648 coupled simulations, the model demonstrated high predictive accuracy, achieving an R^2 of 0.9875 and a *MAE* of 0.0626 when using transfer learning.

On a different note, Liu et al., in [38], developed two DNN models to rapidly predict the nonlinear dynamic response of stiffened plates subjected to near-field UNDEX. The models were trained on a dataset generated from detailed ALE-based LS-DYNA simulations, incorporating variations in charge mass, standoff distance, and geometric properties of plates and stiffeners. The first DNN, with three hidden layers, was used to predict final plastic deformations, while a second, more complex model—with additional neurons and deformation input—was designed to estimate non-uniform effective plastic strain distributions. A third output, the nonlinear displacement–time curves, was also successfully predicted. The models achieved high accuracy (*MSE* below 1%), captured key physical features like strain concentrations and dynamic oscillations, and drastically reduced computation time, making the approach promising for real-time applications in marine structural safety assessment.

Following the work of Liu et al., Ren et al. proposed an ML-based method to predict the damage response of stiffened plates subjected to contact UNDEX scenarios [37]. The model was trained on a dataset generated via detailed ALE-based LS-DYNA simulations, varying plate and stiffener thicknesses, explosive charge mass, and standoff distances. The framework explores the impact of the number of hidden layers, neuron distribution, and network structure on predictive performance. A single DNN with three hidden layers was found essential to accurately capture the complex nonlinear behavior driven by FSI and material plasticity. The method predicts damage borders, plastic deformations, and damage dimensions with high fidelity, achieving consistency rates up to 99.4% when compared with high-resolution FE simulations, previously validated by experiments.

Thus, Wang et al. proposed an improved DNN framework to predict the structural response of ring-stiffened cylindrical shells subjected to far-field UNDEX [46]. Three multi-output DNN models were trained on a dataset of over 2200 finite element simulations performed in ABAQUS, with input features including charge mass, standoff distance, detonation depth, and geometric parameters of the shell and stiffeners. The models predicted plastic deformation and strain of both shell and stiffeners. Grid search method was used to optimize the network topology and dropout rate. The DNN approach outperformed the decision tree, and KNN methods, achieving *MAE* values below 4% and R^2 values above 0.91, showing strong generalization capabilities and significant computational efficiency for rapid assessment of structural integrity in UNDEX scenarios.

In a similar vein, Li et al. [118], developed a single DNN model to predict the dynamic displacement response of target plates subjected to UNDEX, based on numerical data generated through ALE-based LS-DYNA simulations. The network architecture includes two hidden layers and is trained using features such as plate thickness, explosive mass, standoff distance, and spatial coordinates of 121 monitoring points. A custom loss function that combines *MSE* and relative error was designed to improve spatio-temporal prediction accuracy. The DNN achieved an R^2 value of 0.994 and high prediction accuracy on the test set. By expanding the original 125 simulation conditions to over 9000 using the trained model, the authors generated high-resolution response maps that enhance the understanding of deformation trends and provide valuable support for underwater weapon design and protection strategies.

Zhou et al. [119], developed a single ANN to predict the maximum deflection of reinforced cylindrical shells subjected to non-contact UNDEX. The input features include explosive charge mass, standoff distance, and reinforcement plate thickness, while the output is the peak deflection extracted at the end of the first bubble pulsation cycle. The training dataset was generated via 48 CASA simulations in ABAQUS suite, and the ANN architecture consists of a single hidden layer with five neurons. The model achieved high accuracy, with R^2 values above 0.97 on both training and test sets (*MAE* equal to 0.0057, *RMSE* equal to 0.0075), offering a fast and reliable tool for damage assessment and structural protection design in naval applications.

Moving to a different perspective, Nayak et al. [22], developed a ML framework to predict the near-field UNDEX response of coated composite cylinders. Due to the lack of large experimental datasets and the need for physically consistent models, they proposed a hybrid strategy integrating ML with high-throughput multiscale FEM simulations. A comprehensive dataset was generated by varying material properties, coating thickness, and explosive parameters, resulting in over 3800 data points. A single ANN was trained on this dataset to predict structural response metrics. To enhance the interpretability of their NN, SHAP (SHapley Additive exPlanations) values were used to assess feature importance. SHAP is a model-agnostic interpretability

technique based on cooperative game theory, which attributes contributions of each input to the final output by computing Shapley values. The ML model exhibited excellent predictive accuracy, and the approach demonstrated strong agreement with experimental results, highlighting the potential of combining physics-based simulations and ML for efficient, informed design of blast-mitigating composite structures.

In a similar study, Zhang et al. [120] developed a single DNN to predict key physical parameters in simplified UNDEX scenarios, such as cavitation inception time, peak momentum time, and momentum transfer coefficient. The structural system, modeled as two rigid plates connected by a spring and a dashpot, was subjected to planar UNDEX shock waves. The DNN was trained using analytical and numerical results obtained from Laplace transform solutions and Runge–Kutta integration. Input features included stiffness, damping, and FSI parameters. The model achieved high accuracy, with training losses *MSE* below 0.0104%, and successfully replicated trends observed in both validation data and analytical solutions. This work demonstrates the capability of NNs to reduce computational effort in parametric studies of FSI problems.

Other authors, in [121], proposed a DNN-based framework to predict the damage responses—specifically the fractured domain and plastic deformations—of ship cabins subjected to contact UNDEX scenarios. A dataset of 120 ALE-based LS-DYNA simulations was used to train the models, with varying charge masses, standoff distances, and attack angles. A grid search algorithm was employed to systematically optimize hyperparameters, including the number of hidden layers, neurons per layer, and activation functions [122]. Additionally, three new physically derived input features (explosive radius, water depth, and standoff ratio) were introduced to improve prediction efficiency. The optimal model architecture used five layers for fractured domain classification (binary accuracy equal to 99.5%), and four layers for plastic deformation regression (*MAE* equal to 0.0237). The approach significantly improved optimization efficiency (up to 20.5%) and reduced reliance on trial-and-error for network design.

Ma et al. [123], proposed a single ANN-based model to predict the peak pressure at the coupling center of UNDEX generated by two equal-mass spherical charges detonating simultaneously. A total of 123 numerical simulations were conducted using ANSYS AUTODYN suite, varying charge mass and detonation distance. The dataset was log-transformed and normalized before training. The optimal network architecture was selected through systematic testing to minimize *MSE* metric. The ANN achieved a *MSE* of 0.38% on the training set and 0.52% on the test set, outperforming a physics-based formula derived from dimensional analysis. This work demonstrates that ANNs can offer higher accuracy with smaller datasets for shock wave pressure prediction in multi-source UNDEX scenarios.

On a different note, He et al. [124] developed a DNN model to predict the deformation of ship hull bottom plates subjected to near-field UNDEX, using a dataset generated from 40 ALE-based finite element simulations with varying TNT-charge masses and standoff distances. The model takes as input the charge mass, detonation distance, and coordinates on the bottom plate, and outputs the predicted displacement. A grid search was used to optimize the number of layers, neurons, and activation functions, with the best performance achieved by an 8-layer network with 15 neurons per layer. The DNN accurately reproduced complex multi-peak deformation patterns induced by the interaction of shock waves, bubble pulsations, and water jets, achieving *RMSE* below 5.2%, and providing a fast alternative to time-consuming simulations for structural damage assessment.

In the study presented in [125], the authors propose a DNN solver for predicting the shock response spectrum (SRS) resulting from UNDEX, with a focus on improving both computational speed and accuracy. The solver is built upon a single DNN architecture and is trained on acceleration data obtained from ALE simulations. A key innovation lies in the use of an adaptive threshold selection mechanism that partitions the input frequency range, enabling the DNN to independently learn low- and high-frequency features. By leveraging the feature extraction capabilities, the model achieves high fidelity in replicating SRS outputs, significantly reducing the computational cost compared to traditional methods. The application of L2 regularization further enhances generalization and prevents overfitting, making the DNN-based solver a promising tool for rapid and accurate SRS prediction in complex UNDEX scenarios.

In [126], although the focus is on the application of Long Short-Term Memory Networks (discussed in the next section), a DNN is also implemented for comparison. This network, described by Fang et al., is part of a DL-based SHM framework for concrete gravity dams subjected to UNDEX. Specifically, the DNN is employed to further refine the assessment of damage levels, by classifying the damage status of the dam based on extracted damage indicators like peak vibration velocity and domain frequency, showing robust performance with an average classification accuracy of 83.33%.

Although the focus of the work by Li et al. [127] was on the Leave-One-Out eXtreme Gradient Boosting (LOO-XGBoost) algorithm, the authors also employed a DNN model to achieve the same goal of dynamic response prediction for underwater explosive vessels. This ML model used inputs such as explosive charge, hydrostatic pressure, and measurement points on the container, with the output being the predicted dynamic strain response. While the DNN model showed competitive results, with an R^2 of 0.87 and

an *RMSE* of 0.62, the LOO-XGBoost algorithm ultimately outperformed it in terms of prediction accuracy and computational efficiency (see dedicated paragraph for the description of the latter model).

In the study by Chen et al. [128], a DNN model was used to predict the boundary of the UNDEX bubble and the free surface. The inputs to the DNN included parameters such as buoyancy, bubble-free surface distance, and bubble-sidewall distance, with the output being the spatial position of the gas–liquid interface (bubble and free surface boundary). DNN demonstrated high performance in capturing the complex nonlinear relationships in the bubble's dynamics, particularly in regions where the bubble's curvature changes abruptly. The model showed a low *MRE* of 1.01%, indicating its strong ability to fit non-linear data. It was especially effective in predicting the bubble boundary, where other models, including the Random Forest and Extreme Learning Machine, struggled. DNN's accuracy and ability to handle complex, high-dimensional data made it the optimal choice for this task.

In the study by Li et al. [129], a simple ANN model was used to predict the dynamic response of UNDEX vessels. The model, a classical three-layer fully connected NN with 10 nodes inside the hidden layer, included 14 input variables such as time, charge amount, eleven positions of strain gauges and hydrostatic pressure, with the output being the maximum strain of the container. This paper demonstrates that simple models like the ANN, despite their straightforward structure, are not particularly effective for predicting the dynamic response in this complex scenario. The ANN model showed a *MSE* of 3.79 on the test set and a *MAE* of 1.66, which were higher than those of the Classification and Regression Trees model (see dedicated section), the latter considered the focus of this investigation.

Finally, Kong et al. [39], employed a DNN model to predict the fracture and plastic deformation of stiffened plates under UNDEX. The model utilized input variables such as panel thickness, longitudinal bone height, TNT equivalent, and explosion distance. The DNN's performance was impressive, achieving high regression values R^2 of 0.99 for predicting fracture and 0.97 for plastic deformation. These results demonstrate the model's strong capability in accurately assessing the structural response under such explosive conditions.

5.2.1.2 Recurrent Neural Networks (RNNs) and Long Short-Term Memory Networks (LSTMs) Recurrent Neural Networks (RNNs) are a class of ANNs/DNNs specifically designed for processing sequential data, where the order of inputs matters. Unlike traditional ANNs and DNNs, RNNs have a form of internal memory, which allows them to retain information from previous time steps and use it to influence current output predictions [111, 126]. This makes them particularly suited for tasks such as time-series forecasting, speech recognition, and natural language processing, where the context from earlier data points is crucial for understanding current inputs. However, standard RNNs suffer from critical limitations when dealing with long sequences, most notably the vanishing and exploding gradient problems during training. These issues hinder the network's ability to learn and retain dependencies across extended time intervals.

Long Short-Term Memory (LSTM) networks are an advanced type of RNNs specifically designed to learn from sequential and time-dependent data [130]. Traditional RNNs struggle with learning long-range dependencies due to the vanishing gradient problem, which makes them ineffective in capturing patterns over extended sequences. LSTMs solve this issue by incorporating memory cells and a system of gates that control the flow of information through the network.

As shown in Fig. 18, an LSTM network consists of a sequence of LSTM blocks, each receiving input data $\boldsymbol{x}_t$ along with the hidden state $\boldsymbol{h}_{t-1}$ and cell state $\boldsymbol{c}_{t-1}$ from the previous time step. Each block processes the information and outputs an updated hidden state $\boldsymbol{h}_t$ and cell state $\boldsymbol{c}_t$, which are then passed to the next block in the sequence. Zooming into a single LSTM block, it is possible to observe the internal gating mechanism composed of the forget gate f, which decides what information to discard from the previous state; the input gate i, which determines what new information to store, the cell update g, which generates candidate values to add to the memory and finally and the output gate o, which controls how much of the cell state is exposed to the output. These gates allow the network to retain important long-term information and discard irrelevant data dynamically. This architecture enables LSTMs to excel in tasks like runoff forecasting, time-series prediction, and event modeling, where current outcomes are influenced by a sequence of past inputs.

As mentioned previously, in the work proposed by Fang et al., the authors developed a DL-based SHM framework for concrete gravity dams subjected to UNDEX [126]. The framework combines ALE numerical simulations and LSTM-based models (One-layered LSTM, Stacked LSTM, and Attention-LSTM) to predict dynamic responses, specifically displacement and velocity histories, using input acceleration and loading data. Among the models tested, the Attention-LSTM achieved the best performance, particularly in handling multi-point monitoring data under various UNDEX scenarios. The Attention-LSTM model, with its multi-layer architecture and attention mechanism, was able to effectively focus on the most relevant input features, leading to more accurate predictions. It showed superior robustness against noise in the input data and was

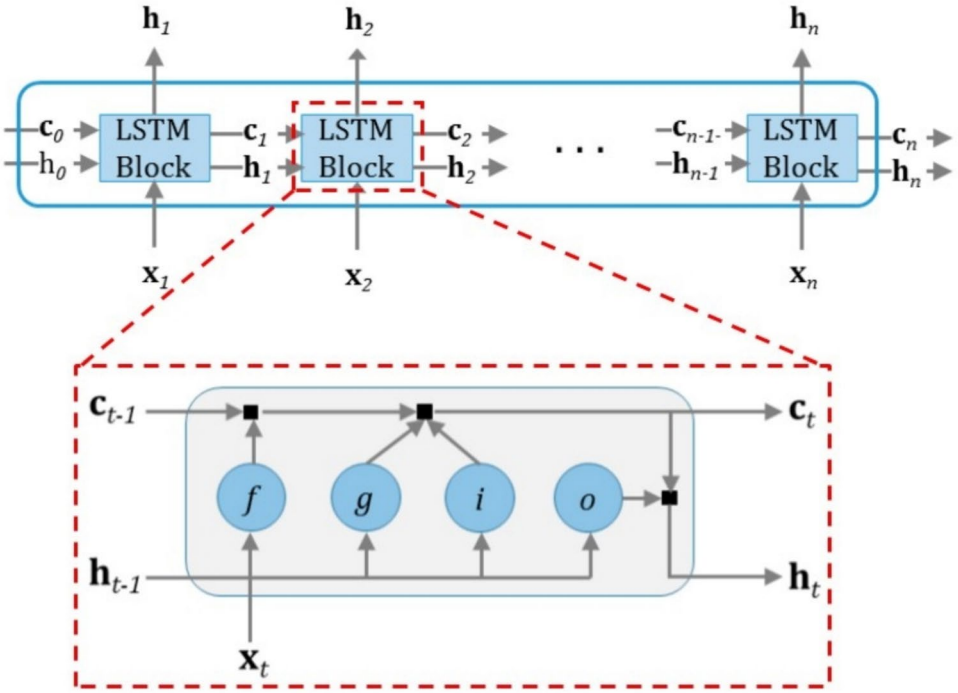

Fig. 18 Scheme of an unrolled Long-Short Term Memory (LSTM), with a magnification of the block structure

able to capture long-term dependencies in the time series data, which enhanced its performance in predicting the structural responses, particularly for complex and nonlinear behaviors. The model outperformed the One-layered and Stacked LSTM models in terms of both training convergence speed and prediction accuracy, particularly for velocity and displacement histories under varying explosion conditions.

Although this work demonstrates promising prospects for this type of model, there are no other applications in the literature, even within the context of marine structures, that explore the use of such advanced LSTM-based frameworks for predicting dynamic responses under UNDEX events.

5.2.1.3 Probabilistic Neural Networks (PNNs) A Probabilistic Neural Network (PNN) is a type of NN based on statistical principles of Bayesian classification and kernel density estimation [131]. As illustrated in Fig. 19, the architecture of a PNN typically includes four layers: the input layer, the pattern layer, the summation layer, and the decision layer. The input layer receives the feature vector $\boldsymbol{X}$ corresponding to a sample that needs to be classified. The pattern layer contains a neuron for each training sample. These neurons compute similarity measures (usually through radial basis functions or Gaussian kernels) between the input vector and each training instance, effectively estimating the probability density function for each class. In the summation layer, outputs from the pattern layer are grouped and aggregated for each class—denoted as $f_A(\boldsymbol{X})$ and $f_B(\boldsymbol{X})$ in the figure—providing a class-wise probability score based on the input

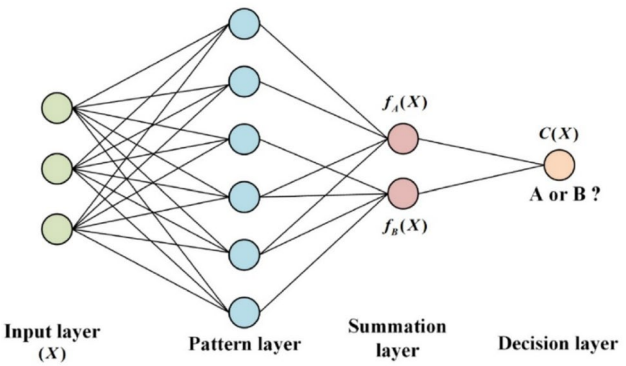

Fig. 19 Illustration of the general framework of Probabilistic Neural Network (PNN). Adapted from [132]

data. Finally, the decision layer compares the aggregated scores $C(\boldsymbol{X})$ and determines the most probable class (e.g., A or B) based on the maximum likelihood criterion [65].

Unlike conventional NNs that rely on backpropagation and gradient descent, PNNs do not require iterative training. Instead, they use non-parametric statistical inference, which makes them particularly fast to train and effective for classification problems with well-separated classes and limited data [125]. Thanks to their fast convergence, robustness to noise, and theoretical foundation in Bayes decision theory, PNNs have been successfully applied in areas such as fault diagnosis, pattern recognition, and medical decision-making. However, a known limitation is their sensitivity to the size of the training set—since each training instance adds

a neuron to the pattern layer, large datasets can lead to high memory and computational requirements. For these reasons, such approaches are rarely adopted in UNDEX applications, where simulations are often computationally expensive, and datasets can quickly grow.

Despite the previous considerations, Guo et al. [65] developed an ML framework based on a different PNN to predict the spectral acceleration response of ships subjected to non-contact UNDEX scenarios. The study introduces two PNN models: one with a single smoothing factor optimized via genetic algorithms, and another with multiple class-specific smoothing factors optimized using particle swarm optimization (PSO). The latter configuration demonstrated improved accuracy, reducing average prediction errors from ~ 25 to ~ 10–15%. The training dataset was built through parametric modeling of ship structures and pure lagrangian FEM simulations under 90 working conditions. The input parameters to the model included the ship's main dimensions, working conditions, and test point positions, while the output was the predicted spectral acceleration. This work represents one of the few applications of PNNs in the context of ship shock environment prediction and highlights the importance of data normalization and optimization strategy on model performance.

5.2.1.4 Physics-Informed Neural Networks (PINNs) The structure of a generic Physics-Informed Neural Network (PINN) is illustrated in Fig. 20. PINNs are an emerging class of DL models designed to embed physical laws directly into the training process of a NN [133]. Unlike traditional data-driven networks, which learn purely from observations, PINNs incorporate governing equations, initial conditions, and boundary conditions into the loss function, enabling the network to approximate physically consistent solutions [95].

As shown in Fig. 20, a standard NN with weights and biases maps inputs $\boldsymbol{x}$ to outputs $\boldsymbol{y}_{pred}$, generating a predicted output vector. The loss function $\mathcal{L}$ that needs to be minimized in a PINN is composed of two key components: $\mathcal{L} = \mathcal{L}_f + \mathcal{L}_{pred}$, where $\mathcal{L}_{pred}$ quantifies the difference between predicted outputs and known data (e.g., measurements), and is typically computed as a norm, while $\mathcal{L}_f$ represents the residuals of the governing physics, including differential equations, initial conditions, and boundary constraints. It ensures that the learned solution is consistent with the underlying physical model [95].

The use of automatic differentiation [134], a key technique in modern DL frameworks (e.g., TensorFlow, PyTorch), allows for efficient computation of the necessary spatial and temporal derivatives of the network output. This enables PINNs to enforce even high-order PDEs within their training loop without the need for traditional discretization schemes.

Recently, for the first time in UNDEX-related problems, Huang et al. introduced a physics-informed, data-driven cavitation model for compressible multiphase flows governed by a polynomial Mie–Grüneisen EOS [95]. The authors employed a PINN trained on both governing physical equations and experimental data from the SESAME EOS library [135] to improve the modeling of unsteady cavitation in UNDEX scenarios. The model integrates physical constraints via differential equations and corrects them using sparse but high-fidelity experimental data. The resulting NN-based EOS successfully captures nonlinear cavitation behavior, maintains pressure and density positivity, and overcomes limitations of classical one-fluid models in high-pressure environments. Numerical validations in one-, two-, and three-dimensional explosion cases demonstrate enhanced accuracy and stability over traditional approaches. This study highlights the strong potential of

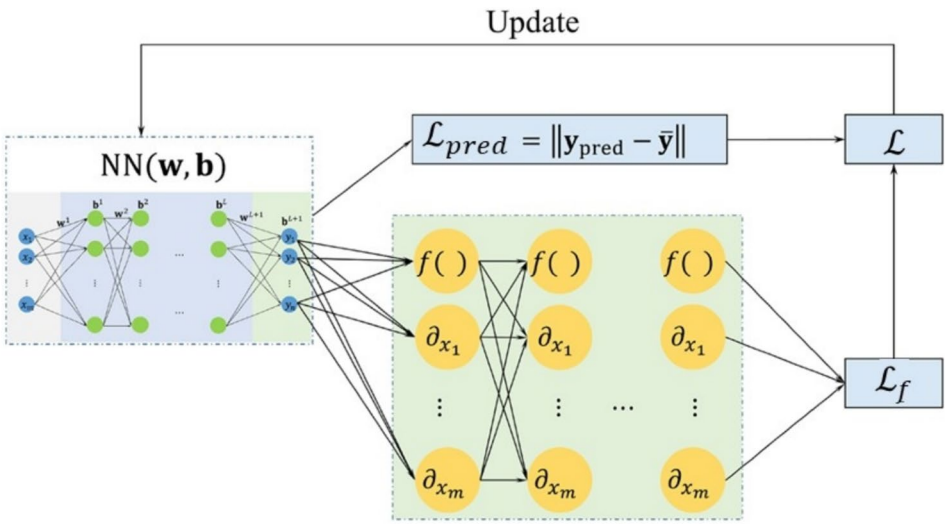

Fig. 20 Illustration of the general framework of Physics-Informed Neural Network (PINN). Adapted from [133]

PINNs in UNDEX modeling, demonstrating their capability to incorporate complex physical laws while leveraging sparse experimental data—making them a promising tool for improving predictive accuracy in highly nonlinear, multiphase explosive environments.

Despite the novelty and promising results of this approach, several limitations are also highlighted in Huang et al.'s study. First, while the model demonstrates strong accuracy in 1D, 2D, and 3D settings, its application is limited to EOS modeling for cavitation phenomena rather than full structural response prediction under UNDEX. Moreover, training PINNs remains computationally expensive, particularly when extended to high-dimensional problems or when incorporating complex boundary geometries. The scarcity of high-quality experimental data further challenges the generalization capabilities of PINNs in realistic UNDEX environments. These limitations underscore the early stage of PINN application in this domain and highlight a clear gap in the literature: there is a need to extend PINNs toward broader structural applications in underwater explosions, including fluid–structure interaction and damage prediction, where physical constraints are essential but data is limited.

5.2.1.5 Extreme Learning Machine (ELM) Extreme Learning Machine (ELM) is a learning algorithm designed for single-layer NNs (SLFNs). Unlike traditional NNs where all weights are adjusted iteratively through specific algorithms, ELM assigns random weights to the input layer and analytically computes the output weights in a single step, typically using the Moore–Penrose pseudoinverse [136]. This approach drastically reduces training time, making ELM extremely efficient for large datasets or real-time applications.

Despite its simplicity, ELM has demonstrated excellent generalization capability in both regression and classification tasks. Its effectiveness depends on the selection of activation functions and the number of hidden nodes, which must be tuned carefully. Due to the absence of iterative tuning, ELM is non-iterative, non-gradient-based, and robust to local minima problems that affect standard backpropagation networks.

In engineering applications, including those related to SHM and dynamic response prediction, ELM has been used for rapid modeling when computational efficiency is a priority [128]. However, its reliance on random initialization can introduce variability in performance, and it may not reach the same accuracy as deeper or more complex architectures like DNNs or LSTM.

In the study by Chen et al. [128], the ELM model was used to predict the boundary of the UNDEX bubble and the free surface. The input variables for the ELM model included buoyancy, bubble-free surface distance, and bubble-sidewall distance, while the output was the spatial position of the gas–liquid interface. The ELM showed a *MRE* of 1.35%, which, while acceptable, was higher compared to the DNN model, which achieved an *MRE* of 1.01%. Despite its faster training speed and fewer hyperparameters, ELM exhibited higher errors in predicting both the bubble and free surface boundaries, particularly in regions with rapid curvature changes. Nevertheless, ELM was selected as the optimal model for predicting the free surface boundary due to its efficient training process, but DNN outperformed it in terms of overall accuracy. This is the only case found in the literature where ELM was applied to predict UNDEX features.

5.2.2 Decision Trees and Tree-Based Ensemble Methods

Tree-based models are a cornerstone of supervised learning due to their interpretability, flexibility, and strong performance across both classification and regression tasks. These qualities make them particularly valuable in UNDEX-related problems, where understanding complex dynamics like material responses to underwater explosions is crucial. In this section, we outline the foundational Decision Tree (DT) algorithm and explore two of its most widely used ensemble extensions: Random Forest and XGBoost, highlighting their effectiveness in tackling the challenges posed by such complex, nonlinear environments.

5.2.2.1 Decision Trees (DT) Decision Trees (DT) are versatile and non-parametric supervised learning algorithms commonly used for both classification and regression problems. They operate by recursively partitioning the input space into subsets based on feature values, building a tree-like structure that is composed of a root node, internal decision nodes, branches, and leaf nodes, as depicted in Fig. 21. Each internal node applies to a decision rule (e.g., a threshold on a feature), guiding the data down the tree, until it reaches a leaf node that provides the final prediction [137].

One of the main strengths of DTs lies in their interpretability: unlike many "black-box" models, DT allows users to visually trace the logic behind each prediction. This makes them ideal for applications where model transparency and feature importance are essential. Additionally, DT can naturally handle both numerical and categorical data without requiring feature scaling or normalization, and they are robust to datasets with missing values.

From a computational perspective, training a DT involves selecting the best feature and threshold to split the data at each node, using several metrics such as Gini impurity, information gain (based on entropy), or variance reduction (for regression). The goal is to create splits that maximize the homogeneity of the resulting subsets with respect to the target variable.

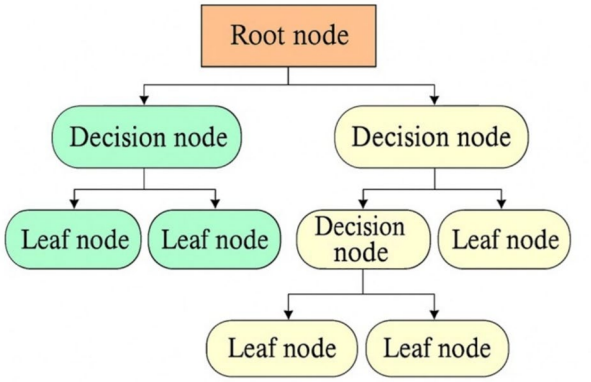

Fig. 21 General schematic of decision tree models (prepared based on [111])

However, a notable limitation of DT is their tendency to overfit the training data, especially when allowed to grow deep without constraints. Deep trees may capture noise rather than underlying patterns, reducing their ability to generalize to unseen data. To mitigate this, techniques such as pre-pruning (e.g., limiting tree depth or minimum samples per leaf) and post-pruning (removing branches that provide little value) are applied.

A first example of DT application in UNDEX-related problems is presented in [128], where the authors applied this model to predict the collapse patterns of bubbles subjected to UNDEX. In this case, it was applied to classify four types of bubble collapse patterns: sharp-corner jet, rounded-corner jet, annular jet, and weak jet. The model splits the data into branches based on input parameters such as buoyancy, bubble-free surface distance, and bubble-sidewall distance. The DT model demonstrated good performance, achieving a classification accuracy of 85.5% on the test set. However, it struggled with predicting class 4 (weak jet) due to its small sample size, which led to errors in classifying these patterns. In comparison with other models like Support Vector Machines and K-Nearest Neighbors, the DT model showed strong performance, especially in handling larger, more balanced datasets.

Shifting the focus, Wang et al. developed a DT model for regression to predict the dynamic response of stiffened cylindrical shells subjected to UNDEX loads [46]. Here, the input parameters were the charge mass, standoff distance, detonation depth, and shell thickness, while the output prediction referred to deformation and strain. After hyperparameter optimization using grid search method, the DT model achieved strong performance with a *MAPE* of 0.045 for stiffener deformation, 0.046 for shell deformation, and 0.062 for plastic strain, along with R^2 values of 0.843, 0.851, and 0.823, respectively. While the DT model demonstrated good accuracy in predicting the structural response, it was still outperformed by the DNN model developed by the same authors, which showed higher R^2 values and lower prediction errors.

As shown in the previous examples, classic DT often has limitations when dealing with more complex tasks. To address these challenges, more advanced models such as Random Forests and Gradient Boosted Trees are introduced later, as they significantly enhance prediction accuracy and stability. These ensemble methods combine the outputs of multiple trees, reducing variance and improving robustness to overfitting.

A widely known and foundational implementation of DT is the Classification and Regression Trees (CART) algorithm, introduced by Breiman et al. in 1984 [138]. CART is a binary tree-building methodology that supports both classification and regression tasks. It uses Gini impurity as the default splitting criterion for classification problems and variance reduction (or mean squared error minimization) for regression. One of the defining features of CART is its exclusive use of binary splits at each decision node, simplifying the tree structure while maintaining high interpretability. CART has not only served as the foundation for standard decision tree models, but also as the building block for more advanced ensemble methods, such as Random Forests and Gradient Boosted Trees. Its algorithmic efficiency, combined with its capacity to produce easily interpretable models, has made CART a widely adopted choice in both academic and industrial applications.

The only attempt to use CART for UNDEX predictions is presented in [129], where Li et al. used it to predict the dynamic response of UNDEX vessels. In this case, the CART model was applied to map the relationship between various input variables such as time, charge amount, hydrostatic pressure, and the position of strain gauges, with the output being the maximum strain of a container target. The model was constructed using a recursive binary partitioning process, where data was split into subsets based on the best feature, and a pruning method was employed to prevent overfitting and enhance the model's generalization ability. The CART model demonstrated superior performance compared to the ANN model developed by the same authors, with a *MSE* of 1.42 and a *MAE* of 1.17 on the test set. These results indicate that the CART model was more efficient in predicting the dynamic strain response of the UNDEX vessel, offering better accuracy and stability than simpler models like ANN.

5.2.2.2 Random Forest (RF) By combining multiple DT trained on different subsets of data, Random Forest (RF) enhances both the robustness and predictive accuracy of standard DT models [128] (Fig. 22). This ensemble learning technique is particularly effective when dealing with large datasets and capturing complex, nonlinear relationships

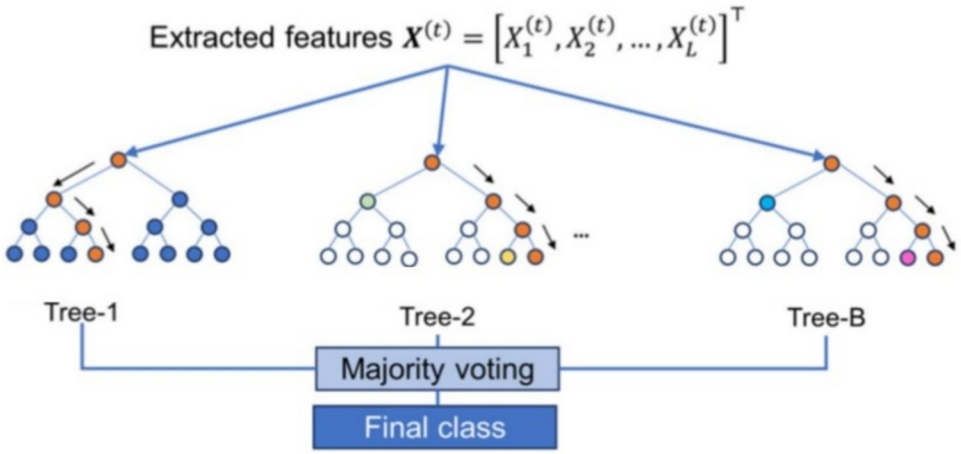

Fig. 22 Random Forest (RF) ML algorithm scheme. Adapted from [112]

among input variables. In the context of UNDEX applications, RF models can be employed to classify or predict structural responses—such as damage categories, failure modes, or pressure thresholds—based on features including explosive charge parameters, geometric configurations, and material properties of the affected structures.

An RF can be trained on a dataset derived from simulated or experimental blast scenarios, where each instance contains descriptors, such as charge weight, standoff distance, detonation depth, and target geometry, along with the observed outcome (e.g., extent of plastic deformation or presence of structural failure). Once trained, the model can be used to forecast the likely response of a structure subjected to a new loading condition, supporting both design optimization and rapid assessment during early-stage evaluations or post-incident diagnostics. The performance of RF models in such settings is typically evaluated using standard regression and classification metrics, such as the R^2, *RMSE*, *MSE*, and *MAE*.

Liu et al. [139], proposed a ML framework to rapidly predict the maximum deformation of ship hull girders subjected to near-field UNDEX. The authors employed a hybrid numerical–data-driven approach, where blast loads were calculated using the Runge–Kutta Discontinuous Galerkin (RKDG) method and applied to ABAQUS CASA simulations to generate training data. A regression model, based on RF, was trained on a dataset including variables such as explosive mass and standoff distance. The RF model showed strong performance in predicting deformation, with a relatively low *RMSE* of 10.31, and a high R^2 of 94%. It achieved a relative error of 10.38%, indicating its suitability for deformation prediction in structural safety assessments under UNDEX scenarios.

In the study by Chen et al. [128], the RF algorithm was employed to predict the boundary of the UNDEX bubble and the free surface. The input variables for the RF model included parameters such as buoyancy, bubble-free surface distance, and bubble-sidewall distance, while the output was the spatial position of the gas–liquid interface (bubble and free surface boundary). As already mentioned, the performance of RF was compared with other regression models, including DNN and ELM. The RF model showed relatively weaker performance in capturing complex, nonlinear relationships, particularly in regions where the bubble's curvature changes significantly. The model achieved higher errors in predicting both the bubble and free surface boundaries compared to DNN and ELM. For instance, the RF's *MRE* was higher, and it struggled with capturing fine details such as the jet velocity, which DNN could predict more accurately. Nonetheless, the RF model still provided valuable insights but was ultimately outperformed by DNN, which showed superior performance in predicting bubble boundaries with lower errors and better robustness.

5.2.2.3 XGBoost XGBoost (eXtreme Gradient Boosting) is a highly efficient and scalable implementation of gradient boosting algorithms, first introduced by Tianqi Chen in 2016 [132]. It has rapidly gained popularity in both academia and industry due to its superior predictive accuracy, computational speed, and flexibility in handling structured data. XGBoost operates by combining multiple weak learners, typically CARTs, into a single strong ensemble model, where each new tree is trained to correct the residual errors of the previous ones. XGBoost differs from traditional gradient boosting in several ways: it uses a second-order Taylor expansion of the objective function for more precise approximation, it includes regularization terms to penalize model complexity and avoid overfitting, it allows for missing data handling and incorporates column subsampling, improving performance and generalization and finally it supports both tree-based and linear base learners, offering flexibility in model design.

Additionally, XGBoost includes advanced system optimization features such as parallel computation, cache

awareness, and out-of-core learning for large datasets. These make it especially suitable for high-performance environments and real-time predictive systems.

Given its robustness and ability to handle nonlinear interactions, noisy data, and limited sample sizes, XGBoost is widely regarded as one of the most effective algorithms for regression and classification problems in engineering, including dynamic modeling of structures under explosive loads.

As already mentioned previously, Liu et al. [139] employed a hybrid numerical–data-driven approach to predict the maximum deformation of ship hull girders subjected to near-field UNDEX, using inputs such as explosive mass and standoff distance. The outputs of the model were the predicted deformations of the hull girders. Among the regression models tested, XGBoost outperformed RF in terms of prediction accuracy. XGBoost achieved a lower *RMSE* of 27.67 compared to RF's 50.31, a higher R^2 of 96% versus RF's 94%, and a smaller relative error of 6.25% compared to RF's 10.38%, confirming its suitability for accurate and efficient deformation prediction in structural safety assessments under UNDEX scenarios.

Another application of the XGBoost model is presented in [127], where Li et al. proposed a dynamic response prediction model for underwater explosive vessels based on the Leave-One-Out XGBoost algorithm. The model was developed to address the challenges of small sample sizes, unclear feature relationships, and limited effective data in UNDEX experiments. The primary inputs to the model included the explosive charge, hydrostatic pressure, and measurement points on the container, while the output was the predicted dynamic strain response. The model was compared to several ML algorithms, including Support Vector Regression and DNN. The LOO-XGBoost model demonstrated superior performance, with an R^2 of 0.9967 and a *RMSE* of just 0.0808, significantly outperforming the other models. These results highlight the effectiveness of LOO-XGBoost in providing accurate predictions of the dynamic response of underwater explosive vessels, even with small datasets, and offer valuable insights for future underwater explosion testing and container design.

5.2.3 Instance-Based and Distance-Based Learning Algorithms

This section covers models that make predictions by directly relying on the similarity between observations, rather than explicitly learning a function through the optimization of internal parameters, as is the case in NN- or tree-based models. In these approaches, the model does not attempt to generalize by finding an underlying function; instead, it evaluates how closely new instances resemble the instances in the training dataset. The predictions are made based on the relationships or distances between the input data points, which makes these algorithms highly intuitive and effective in certain types of problems, particularly where the data structure is complex or hard to model explicitly.

5.2.3.1 K-Nearest Neighbor (KNN) The K-Nearest Neighbor (KNN) algorithm, first introduced in 1951, is a simple yet highly effective method. Over the years, numerous variations of KNN have been applied across a wide range of domains, including text classification, facial recognition, and various other problem-solving tasks [140]. The fundamental principle of KNN is to predict the output for a new data point by examining the K most similar instances—i.e., the nearest neighbors—in the training dataset. Depending on the task at hand, this may involve either estimating a continuous value or assigning a discrete category to the input [112]. In essence, the method is used to infer an outcome for a variable not present in the original dataset, based on the behavior of similar, previously observed data. In the case of K-Nearest Neighbors Regression (KNNR), the algorithm begins by computing the distance—typically Euclidean—between the new input (covariate) and all other covariates in the dataset. This distance is given by the general formula $d_i(x_i, \boldsymbol{x}) = \sqrt{(x_1 - \boldsymbol{x})^2 + (x_2 - \boldsymbol{x})^2 + \ldots + (x_n - \boldsymbol{x})^2}$. Next, the algorithm identifies the K nearest covariates by selecting those with the smallest calculated distances from the new input. The corresponding response values of these K neighbors are then averaged to estimate the output. The predicted response $\hat{y}$ is computed using the formula $\hat{y} = \frac{1}{k} \cdot \sum_{y_i \in C} y_i$. This approach assumes that covariates located close to each other in the feature space are likely to have similar response values. Given a dataset with n covariates. $X = x_1, x_2, \ldots, x_n$ and corresponding responses $Y = y, y_2, \ldots, y_n$, the KNN algorithm exploits this local similarity to infer the unknown outcome. In some cases, weighted versions of the algorithm are used, where the contribution of each neighbor to the final prediction is scaled by a weight. These weights are often based on the inverse of the distance or derived from a Gaussian distribution, so that closer neighbors exert more influence on the predicted value. Nevertheless, uniform weighting—where all K neighbors contribute equally—remains the most adopted strategy.

In the study proposed in Wang et al. [46], employed the KNN ML model to predict the dynamic response of stiffened cylindrical shells under UNDEX loads. The KNN model utilized input parameters such as charge mass, standoff distance, detonation depth, and shell thickness to predict outputs like deformation and strain. After optimizing the model with hyperparameter tuning using the grid search method, KNN achieved relatively good performance with *MAPE* of 0.036 and R^2 of 0.862 for stiffener deformation,

0.039 and 0.874 for shell deformation, and 0.056 and 0.849 for plastic strain predictions. The results show that while KNN provides accurate predictions, it still lags the DNN model (developed by the same authors) in terms of predictive accuracy.

Finally, in [128], a KNN model was utilized to classify the collapse patterns of bubbles subjected to UNDEX. In this case, the input features included parameters such as buoyancy, bubble-free surface distance, and bubble-sidewall distance, and the output was the predicted collapse pattern. KNN showed good performance in classifying the bubble collapse patterns, but it faced challenges with imbalanced datasets, particularly when predicting the "weak jet" class, which was underrepresented. While KNN is generally known for its simplicity and effectiveness in capturing local patterns, its performance can degrade in high-dimensional spaces or when the data contains noise.

5.2.3.2 Support Vector Machine (SVM) and Support Vector Regression (SVR) Support Vector Machines (SVM) are powerful supervised learning algorithms commonly used for classification, regression, and outlier detection tasks [58]. Introduced by Cortes and Vapnik in 1995, SVM is grounded in statistical learning theory. The fundamental concept of SVM involves identifying the optimal hyperplane that best separates different classes of data in a high-dimensional space. This hyperplane maximizes the margin—the distance between the closest data points (known as support vectors) and the decision boundary (Fig. 23).

For regression problems, the SVM framework is extended into Support Vector Regression (SVR). Unlike traditional regression models that aim to minimize the prediction error, SVR attempts to fit the best line within a predefined margin of tolerance (ϵ), disregarding errors that fall within this margin. This formulation enhances robustness, especially when dealing with small datasets and high-dimensional feature spaces [39].

A key advantage of SVR is its insensitivity to the dimensionality of the input space, allowing it to generalize

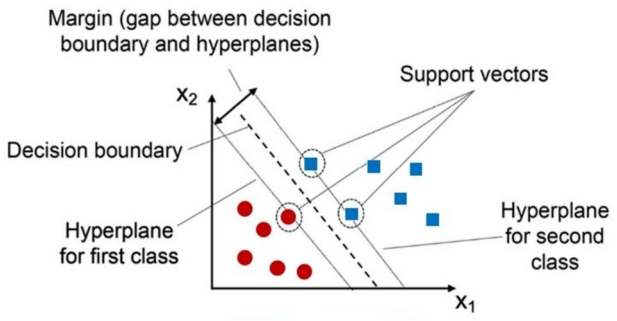

Fig. 23 Support Vector Machine (SVM) general scheme. Adapted from [111]

well even with limited training samples. It has demonstrated high accuracy and generalization capability, especially when the underlying relationships between variables are nonlinear. These nonlinearities are captured through kernel functions, such as radial basis function (RBF), polynomial, or linear kernels, which project the data into higher-dimensional spaces where linear separation or fitting becomes feasible. However, SVM and SVR are not without limitations. They can be computationally intensive, particularly during training, and they require careful tuning of hyperparameters, such as the kernel type and regularization parameters. Additionally, the models tend to be less interpretable compared to tree-based methods, and they may struggle with very large datasets or when noisy data and outliers are present [58].

Kong et al. [39], employed both the SVM and SVR models for predicting the structural responses of stiffened plates subjected to UNDEX. The SVM model was applied to determine the failure criterion, specifically distinguishing between fractures and plastic deformations. This model achieved a high training accuracy of 99.4%, indicating its effectiveness in classifying different structural failure scenarios. The SVR model, based on SVM, was used to predict both the fracture area and plastic deformation. For fracture prediction, the SVR model achieved a R^2 of 0.96 on the training set and 0.96 on the test set, demonstrating strong predictive performance. For plastic deformation, the SVR model showed an R^2 of 0.90 on the test set, which is slightly lower but still indicates a good fit. These results indicate that while the SVM and SVR models are accurate and reliable, the DNN model outperformed them in terms of predictive accuracy for both fracture and deformation, as demonstrated by the higher R^2 values in the DNN model (0.99 and 0.97). Nonetheless, the SVM and SVR models remain valuable tools due to their efficiency and strong performance in these tasks.

Finally, in [127], the SVR model was employed to predict the dynamic response of underwater explosive vessels. The input variables for the SVR model included factors such as explosive charge, hydrostatic pressure, and the location of measurement points on the vessel, with the output being the strain at those points. When compared with other models like the LOO-XGBoost, SVR showed lower performance in terms of prediction accuracy. Specifically, the R^2 value for SVR was 0.9104 for measurement point 1 and 0.7681 for measurement point 2, which was significantly lower than the LOO-XGBoost model's R^2 of 0.9967 and 0.9985, respectively. Additionally, the *RMSE* for SVR was 0.4221 for measurement point 1, which was much higher than that of the LOO-XGBoost model (0.0808), indicating that SVR was less accurate in predicting the vessel's dynamic response. Despite this, SVR remains a valuable tool in certain UNDEX scenarios,

particularly where computational efficiency and simplicity are prioritized.

5.2.4 Advanced Learning Strategies

5.2.4.1 Transfer Learning (TL) in Supervised Models Transfer Learning (TL) is an ML technique in which a model developed for a particular task is reused as the starting point for a model on a second, related task [141]. Rather than training a model from scratch, TL leverages the knowledge learned by a pre-trained model—usually on a large dataset—allowing it to generalize and perform effectively on a new task with limited data. This approach is especially powerful in scenarios where labeled data is scarce or expensive to obtain, as it significantly reduces the computational cost and training time while improving performance. Commonly used in computer vision and natural language processing, TL typically involves taking an ANN or DNN trained on a large dataset (e.g., ImageNet or BERT), freezing some of its layers, and fine-tuning the remaining layers on the target dataset [141]. Beyond NNs, the concept can also be applied more broadly, including in RL and semi-supervised learning settings, where knowledge acquired in one environment or task can enhance learning in another. By bridging gaps between domains, TL is a cornerstone in building efficient and scalable AI and ML systems.

For the first time in the UNDEX field, Bardiani et al. applied TL to predict the explosive mass in UNDEX events using a previously developed DNN [29]. Starting from a previously trained classification model that predicted the charge location [25], the authors repurposed its architecture to perform a regression task aimed at estimating the charge mass. The dataset was expanded from 108 to 648 high-fidelity CEL simulations in MSC Dytran suite by introducing charge mass variability. By transferring the weights of the shared hidden layers from the original DNN, the new model achieved faster convergence, lower error metrics, and improved generalization, compared to training from scratch. This work demonstrates the potential of TL in reducing computational costs while preserving high predictive accuracy, even with limited datasets, and highlights its practical applicability for real-time onboard estimation of explosive characteristics.

5.2.4.2 Ensemble Learning (EL) Ensemble Learning (EL) refers to a class of ML techniques that aims to improve predictive performance by combining the outputs of multiple base models [142]. Rather than relying on a single algorithm, EL methods integrate the predictions of several "weak" or moderately accurate models to generate a final decision that is typically more robust and accurate. This approach is based on the idea that a group of diverse models, when aggregated, can outperform any single constituent model, especially in terms of generalization to unseen data. Several attempts have been made to apply this strategy to UNDEX problems, where the complexity and variability of the data present significant challenges for individual models. For example, in [128], the authors employed a combination of different ML models to improve the accuracy of bubble collapse pattern classification. By leveraging the strengths of multiple algorithms, they created a fusion model that integrated SVM, KNN, and DT models. The input features to the model included parameters such as buoyancy, bubble-free surface distance, and bubble-sidewall distance, while the output was the predicted collapse pattern of the bubble, categorized into four types: sharp-corner jet, rounded-corner jet, annular jet, and weak jet. This ensemble approach effectively addressed the limitations of individual models, particularly in cases where datasets are imbalanced, and certain classes are underrepresented. The fusion model achieved 100% classification accuracy across all four bubble collapse patterns, demonstrating the power of combining models.

6 Summary of ML Prediction Models and Their Main Features

Table 2 provides a detailed summary of the existing literature concerning the application of ML tools for UNDEX predictions. For each study, the table reports: (i) the reference to the paper, (ii) the taret structure examined, (iii) the material of the structure under investigation, (iv) the type(s) of ML models employed, (v) whether the ML model was used for a regression or classification task, (vi) the type of database adopted to train the model along with the software utilized to create the dataset (if it was generated numerically), (vii) the dataset generation strategy (ALE, CEL, CASA, BEM, etc.), and (viii) whether the numerical model was validated against experimental data. Overall, this table is intended to offer a comprehensive perspective on how ML approaches have been integrated into UNDEX prediction tasks, highlighting the diversity in methodologies, simulation frameworks, and validation practices across different contributions in the field.

It is important to note that all the investigations found in the literature are based on simplified or scaled structural models; no study to date has applied ML techniques to full-scale structures under UNDEX loading, highlighting a current limitation in the practical deployment of these approaches.

In Table 3, the details of the ML models applied to UNDEX prediction tasks are presented. This table outlines the inputs, outputs, and dataset dimensions for various ML models used in UNDEX prediction. Additionally, it highlights whether data augmentation techniques were applied

Table 2 Overview of literature on the application of ML tools for UNDEX predictions

Paper	Objective	Structure examined	Material	Type of ML model	Regression and/or classification	Type of database (software)	Dataset generation strategy	Validation	Year
[37]	Prediction of complex damage responses of stiffened panels under near-field UNDEX and analyze the influence of activation functions and optimizers	Horizontal stiffened plates	Steel	Single DNN (double step prediction)	Regression	Numerical (LS-DYNA)	ALE	Experiment in [76]	2022
[22]	Prediction of the response of coated composite cylinders subjected to near-field UNDEX	Coated composite cylinders	Composite	Single ANN	Regression	Multiscale numerical (LS-DYNA and ABAQUS CAE)	ALE	Experiment in [98] and [143]	2022
[24]	Correlate coupled and uncoupled simulations for near-field UNDEX to exploit fast uncoupled results	Vertical unstiffened plates	Steel and aluminum alloys	Single DNN	Regression	Numerical (MSC DYTRAN)	CEL	Experiment in [103] and [12]	2025
[25]	Reconstruct the spatial position of the detonation point in case of seabed reflection for near-field UNDEX	Horizontal unstiffened plates	Steel and aluminum alloys	Single DNN	Classification	Numerical (MSC DYTRAN)	CEL	Experiment in [12]	2025
[29]	TL application to predict the mass of the charge based on a previous ML model in near-field UNDEX	Horizontal unstiffened plates	Steel and aluminum alloys	Single DNN + TL	Regression	Numerical (MSC DYTRAN)	CEL	Not directly validated	2025
[38]	Prediction of nonlinear responses of stiffened plates under near-field UNDEX	Horizontal stiffened plates	Steel	Two DNNs in series	Regression	Numerical (LS-DYNA)	ALE	Experiment in [12]	2022
[39]	Prediction of the plastic deformation and fracture area of stiffened plates under UNDEX	Horizontal stiffened panels	Steel	SVM, SVR and DNN	Classification and regression	Numerical (ABAQUS CAE)	CEL	Experiment in [144]	2023

Table 2 (continued)

Paper	Objective	Structure examined	Material	Type of ML model	Regression and/or classification	Type of database (software)	Dataset generation strategy	Validation	Year
[46]	Prediction of the plastic deformation and strain of stiffened cylindrical shells under far-field UNDEX	Ring stiffened cylindrical shell	Steel	Three DNN, DT and KNN	Regression	Numerical (ABAQUS CAE)	Pure Lagrangian	Experiment in [145]	2024
[95]	Prediction of cavitation in compressible multi-phase flows during UNDEX events	-	-	PINN	Regression	Numerical (in-house code)	Pure Eulerian	Numerical	2025
[139]	Prediction of the deformation of a ship hull girder under underwater explosion	Ship hull girder	Steel	XGBoost and Random Forest	Regression	Numerical (ABAQUS CAE)	CASA	Experiment in [146]	2025
[124]	Prediction of the deformation of a hull structure under near-field UNDEX	Typical double bottom hull structure	Steel	Single DNN	Regression	Numerical (LS-DYNA)	ALE	Experiment in [4] and [147]	2025
[128]	Recognition of bubble collapse patterns and prediction of flow field state from near-field UNDEX	-	-	SVM, KNN, DT, EL, DNN, ELM, RF	Classification and regression	Numerical (in-house code)	BEM	Experiment in [148]	2024
[119]	Damage prediction of reinforced cylindrical structure subjected to non-contact UNDEX	Reinforced cylindrical section	Aluminum	Single ANN	Regression	Numerical (ABAQUS CAE)	CASA	Experiment in [149]	2024
[118]	Prediction of the deformation response of a target plate subjected to near-field UNDEX	Horizontal unstiffened plates	Steel	Single DNN	Regression	Numerical (LS-DYNA)	ALE	Not performed	2024

Table 2 (continued)

Paper	Objective	Structure examined	Material	Type of ML model	Regression and/or classification	Type of database (software)	Dataset generation strategy	Validation	Year
[121]	Prediction of the structural damage (fractured domain and plastic deformations) of ship cabins subjected to contact UNDEX	Ship cabin	Steel alloys	Single DNN	Regression	Numerical (LS-DYNA)	ALE	Experiment in [150]	2024
[123]	Prediction of the peak pressure at shock wave coupling center considering two UNDEX sources	-	-	Single DNN	Regression	Numerical (ANSYS AUTODYN)	Pure Eulerian	Not performed	2017
[126]	Prediction of dynamic response and assessing damage of concrete gravity dam under UNDEX	Gravity dam	Concrete	LSTM and DNN in series	Regression and classification	Numerical (LS-DYNA)	ALE	Experiment in [151]	2023
[125]	Prediction of the Shock Response Spectrum (SRS) of a ship section subjected to UNDEX	Parametrized model of a ship section	Steel	Single DNN	Regression	Numerical	ALE	Not performed	2024
[65]	Prediction of the spectral acceleration at specific points within a ship structure under UNDEX	Surface ship	Steel	PNN	Regression	Numerical	Pure Lagrangian	Not performed	2020
[120]	Prediction of the dynamic response of simplified submerged structures to far-field UNDEX	Parametrized model of a ship	-	Single DNN	Regression	Analytical (Taylor's theory)	–	Not performed	2019
[127]	Prediction of the dynamic response of underwater explosive vessels in cases with limited sample sizes	Underwater explosive container	Steel	XGBoost, SVR and DNN	Regression	Experimental	–	Not performed	2023

Table 2 (continued)

Paper	Objective	Structure examined	Material	Type of ML model	Regression and/or classification	Type of database (software)	Dataset generation strategy	Validation	Year
[129]	Prediction of the dynamic response of underwater pressure vessel under UNDEX	Cylindrical container	Steel	CART and ANN	Regression and classification	–	Experiments	Not performed	2020

and whether the models are considered explainable. The focus is on providing a summary of the key components involved in training and applying these ML models for accurate predictions related to UNDEX events. For more detailed information, readers are referred to the specific references.

7 Practical Guidelines for ML-Based UNDEX Prediction

Based on the systematic literature review and the bibliometric and methodological insights discussed, we propose the following actionable guidelines to support the development of robust and generalizable machine learning models for UNDEX-related tasks.

1. Match the model architecture to data size and task complexity

Deep Neural Networks (DNNs) are suitable for large datasets and complex, highly nonlinear relationships—such as predicting full-field responses or generalizing across varying structural configurations. In contrast, tree-based ensemble models (e.g., Random Forest, XGBoost) are advantageous when data is limited, input features are heterogeneous, or model interpretability and computational efficiency are important (e.g., early-stage damage screening). Consider trade-offs between flexibility and explainability based on application needs.

2. Select input features that are measurable and relevant

Prioritize features that are directly measurable (e.g., strain, acceleration, pressure) or reliably inferable from sensor data, rather than theoretical variables like explosive mass or exact standoff distance. Since the choice of input features remains case-specific, future work should report and justify input selection more systematically. This is a key step toward real-time onboard applications.

3. Choose the problem formulation according to the engineering goal

Decide whether the ML task should be regression (e.g., maximum displacement, stress levels) or classification (e.g., damage category, charge location) based on the nature of the desired output. Aligning the problem setup with the operational objective helps streamline both data preparation and model evaluation.

Table 3 Details of the ML models applied to UNDEX prediction tasks

Paper	Inputs	Outputs	Dataset dimension	Data augmentation?	Explainable ML model?	Performance metrics
[37]	Length of the plate Width of the plate Thickness of the plate Thickness of stiffeners Charge mass Standoff distance	First step Plastic deformations Border of the damaged domain Second step Dimension of the damaged domain of the plate	135 samples	No	No	MRE R^2
[22]	Energy of the explosive Stand-off distance Ratio of coating thickness to the wall thickness of the cylinder Density of the coated laminate	Peak internal energy of the target structure	3837 samples	No	Yes	MSE R^2
[24]	Plate's mass-per-unit-area Explosion type Equivalent plastic strain time history Uncoupled out-of-plane displacement time history	Coupled out-of-plane displacement time history	448 samples	Yes	No	MSE
[25]	First peak pressure Second peak pressure First peak time instant Secon peak time instant Shock arrival time instant Maximum out-of-plane displacement Plate's mass-per-unit-area Distance between plate and seabed Seabed's elastic modulus Plate's elastic modulus	Position of the charge on a 2-D grid	108 samples	No	No	Accuracy Precision Recall F1 score Confusion matrix
[29]	Same as [25]	Explosive mass	648 samples	No	No	Same as [25]
[38]	First DNN Charge mass Standoff distance Thickness of the plate Thickness of the stiffeners Second DNN Final plastic deformation Displacement–time curve	First DNN Final plastic deformations Displacement–time curves Second DNN Effective plastic strain nephograms	95 samples	No	No	MRE
[39]	SVR, SVM and DNN Panel thickness Equivalent charge mass Standoff distance Longitudinal bone height	SVM Failure criterion (fractures or plastic deformations) SVR and DNN Fracture area	625 samples	No	No	Accuracy Precision Recall F1 score Specificity Confusion matrix RMSE
[46]	Charge mass Standoff distance Detonation depth Cylindrical shell thickness Web thickness Flange thickness	Radial and tripping deformation of ring stiffeners Radial deformation of the cylindrical shell Plastic strain	2274 samples	No	No	MSE RMSE MAPE
[95]	Logarithmic transformed density	Logarithmic transformed pressure	Not specified (taken from SESAME dataset [135])	No	No	MSE

Table 3 (continued)

Paper	Inputs	Outputs	Dataset dimension	Data augmentation?	Explainable ML model?	Performance metrics
[124]	Charge mass Standoff distance Coordinate x of the charge Coordinate y of the charge	Deformations of the bottom plate	40 samples	No	No	MSE RAE R^2
[139]	Equivalent charge mass Standoff distance	Maximum deformation of the ship hull girder	45 samples	No	No	MSE
[118]	Charge mass Standoff distance Thickness of the reinforced plate	Maximum deformation of center point of the target plate	125 samples	No	No	MSE
[128]	SVM, KNN, DT and EL Buoyancy parameter Bubble-free surface distance Bubble-vertical sidewall distance DNN, ELM and RF Buoyancy parameter Bubble-free surface distance Bubble-vertical sidewall distance Bubble collapse pattern class	SVM, KNN, DT and EL Bubble collapse pattern class DNN, ELM and RF Gas–liquid interface position (x, y and z) Velocity on the interface Potential of velocity on the interface	228 samples	No	No	Accuracy Precision Recall F1 score Confusion matrix
[119]	Equivalent charge mass Standoff distance Thickness of the reinforced plate	Maximum deflection of the cylindrical shell structure	48 samples	No	No	MAE RMSE R^2
[123]	Charge mass Standoff distance	Peak pressure at shock wave coupling center	123 samples	No	No	MAE RMSE R^2
[126]	LSTM Load history on the upstream surface of the dam Accelerations history in x and y directions Simulated noise DNN Damage indicators	LSTM Vibration velocity histories Displacement histories Damage indicators DNN Damage level (no, slight and severe)	LSTM 800 samples DNN 200 samples	No	No	MSE
[120]	Spring stiffness Fluid–structure factor Damping coefficient	Cavitation time Peak momentum time Momentum transfer coefficient	Not specified	No	No	MAE RMSE R^2
[65]	Charge mass Hydrostatic pressure Measurement points positions	Deformation (strain) at two specific locations	31 samples	No	No	MSE
[121]	Charge mass Standoff distance Attack angle Equivalent charge radius Depth of the charge	Fractured domain Plastic deformations	120 samples	No	No	MAE MSE R^2
[129]	Time history Charge mass Hydrostatic pressure N°11 variables of the position of strain gauge	Maximum strain of container	782 samples	No	No	MSE

Table 3 (continued)

Paper	Inputs	Outputs	Dataset dimension	Data augmentation?	Explainable ML model?	Performance metrics
[127]	Length ship section Breadth ship section Draught ship section Weight of the ship section Charge mass Explosion attack angle Critical distance Impact factor x-coordinate of the measurement point y-coordinate of the measurement point z-coordinate of the measurement point	Spectral acceleration at the specified measurement points	1000 samples	No	No	MSE RAE R^2

4. Apply advanced learning strategies when appropriate

Transfer Learning (TL) is effective when adapting models trained on simpler scenarios (e.g., flat plates) to more complex structures (e.g., stiffened panels), allowing for faster convergence and better generalization with fewer training samples. Ensemble Learning (EL) is useful in improving robustness and accuracy by combining multiple weak or moderate models, especially in presence of imbalanced or noisy datasets.

5. Diversify and validate datasets carefully

Most datasets in this domain are generated through high-fidelity simulations (e.g., CEL, ALE). To improve model reliability, experimental validation is strongly recommended when feasible. Techniques such as data augmentation and synthetic generation via parameter variation should be used to increase variability and reduce overfitting.

6. Use consistent and task-appropriate evaluation metrics

For regression tasks, adopt RMSE, MAE, and R^2; for classification, use accuracy, F1-score, and confusion matrices. Clear and consistent metric reporting is essential for comparing models across studies and applications.

7. Integrate interpretability and physics awareness

Model transparency is essential for safety–critical applications. Use SHAP values, feature importance analysis, and sensitivity studies to understand model behavior. Physics-Informed Neural Networks (PINNs) or hybrid frameworks incorporating governing equations can help enforce physical consistency and enhance trust.

8 Challenges and Future Research Directions

While the ML methods reviewed herein have demonstrated promising results in predicting UNDEX phenomena, several challenges remain that warrant further exploration in this emerging interdisciplinary field. This section outlines these challenges and their corresponding potential directions.

- Although a few studies have explored more sophisticated ML architectures, the majority of current research relies on relatively simple models, primarily standard DNNs. Investigating the performance of state-of-the-art ML models—such as graph neural networks, transformers, or physics-informed architectures—could offer valuable advancements in predictive capability and model robustness for UNDEX-related applications.
- Given the limited availability of large datasets in the UNDEX domain, future research could explore data augmentation strategies—such as physics-based simulations, generative models (e.g., GANs), or domain-informed synthesis—to enhance dataset diversity and improve ML model generalization.
- Hybrid modeling that combines ML with physics-based approaches represents a promising yet underexplored

direction in the UNDEX field. Except for one identified application of PINNs, such integration remains rare and could enhance both accuracy and physical interpretability of predictions.

- Improving the interpretability of ML models in UNDEX applications is a key research direction. Techniques such as feature importance analysis or attention mechanisms can enhance trust and foster wider adoption. Explainable AI (XAI) may also offer insights into the physical drivers behind structural response predictions.
- Collaboration between AI and ML researchers and experimentalists is crucial to validate and refine model predictions in UNDEX studies. The integration of numerical and experimental data remains a critical challenge. Leveraging TL techniques could help bridge this gap by adapting ML models trained on synthetic datasets to real-world experimental scenarios, thereby enhancing model reliability and applicability.
- Current investigations in the application of ML to UNDEX phenomena are mostly limited to simplified or small-scale structural components. This highlights a significant gap between existing research and practical needs, where real-world marine and offshore structures—such as ships—are large and complex. Nonetheless, evidence from adjacent domains (e.g., aeroelasticity, structural health monitoring) suggests that robust and scalable ML frameworks can be developed for complex systems, provided that appropriate strategies such as transfer learning and hybrid modeling are employed.
- A major challenge—closely related to multi-scale modeling and practical deployment—is that many current ML models rely on input parameters that are not directly measurable in real-world scenarios. For example, key variables such as charge mass and standoff distance are often assumed known, while in practice they are rarely available from onboard sensors. This disconnect limits the operational applicability of such models, especially in safety–critical contexts like naval or aerospace applications. Moreover, the selection of input features itself remains an open and unresolved research question. There are currently no standardized guidelines or universally accepted best practices for choosing the most appropriate set of inputs. This is largely because the optimal input space is highly problem-specific, depending not only on the type of structure and the nature of the loading scenario, but also on the available sensor configuration and the ultimate prediction objective (e.g., damage classification, displacement prediction, probability of failure, etc.). Future research should therefore not only prioritize the use of input features that are either directly measurable or reliably inferable from sensor data, but also systematically investigate and document the impact of different input selections on model performance. Such studies would help build a foundation for more generalized frameworks and decision-support tools to guide input selection in diverse application domains.
- Another promising yet unexplored direction involves the use of Graph Neural Networks (GNNs) for structural response prediction under UNDEX loading. Unlike traditional neural networks, GNNs operate on graph-structured data, making them naturally suited for domains like structural mechanics, where finite element models can be represented as graphs—nodes corresponding to mesh points and edges to physical connectivity. In this context, GNNs could be leveraged to learn stress or displacement propagation across the structure, capturing spatial dependencies and local interactions more effectively than fully connected architectures. Furthermore, the inherent inductive bias of GNNs could improve model generalization across different structural topologies, reducing the need for retraining on each new geometry. Although no existing studies have yet applied GNNs specifically to UNDEX problems, their application in adjacent fields such as structural health monitoring suggests a strong potential worth exploring.
- While regression-based models currently dominate the field, classification tasks are gaining traction in UNDEX-related applications, particularly for tasks such as damage localization, blast quadrant identification, or scenario recognition. Future studies should further explore and refine classification strategies, as they offer complementary insights for decision-making under uncertainty.
- Composite structures exposed to UNDEX events exhibit complex multi-scale behaviors, where damage mechanisms can initiate at the microscale and propagate to the structural scale. Future research should explore multi-scale modeling strategies that integrate ML with numerical methods—such as finite element analysis or mesoscale simulations—to accurately capture and predict the response of composites across different length scales under explosive loading.
- A common limitation observed in current ML applications for UNDEX is their poor generalizability beyond the specific conditions used during training. Models often perform well only within the narrow scope of the original dataset but fail when applied to different structural geometries or boundary conditions. However, promising approaches from other complex domains—such as physics-informed learning and domain adaptation—suggest that this limitation can be overcome. This underscores the need for more adaptable models and training pipelines that can generalize across a wider range of configurations without retraining from scratch.
- An additional promising research direction involves extending current ML-based frameworks to account for

cumulative damage and fatigue behavior resulting from multiple far-field UNDEX events, which more closely reflect real operational scenarios and are critical for long-term structural safety assessment.
- Another relevant direction for future research is the use of AI and ML models to infer additional structural responses—such as strain and stress—in regions of the structure where no direct measurements are available, leveraging learned correlations from limited sensor data.
- To address the challenge of limited generalizability, future studies could explore advanced learning paradigms such as multi-task learning, meta-learning, and domain adaptation, which are well-suited to improve model robustness across varying UNDEX configurations and structural conditions.
- Despite the importance of experimental validation, practical limitations such as high testing costs, strict safety regulations, and the scarcity of publicly available data from explosive testing campaigns remain significant barriers to the widespread use of experimental datasets in this domain.
- Recent applications have demonstrated the utility of data augmentation techniques—such as geometric transformations applied to numerical fields—to increase dataset size while preserving physical consistency. Nevertheless, more advanced generative strategies, including GANs, have not yet been explored in this context and could offer powerful tools to create diverse, high-fidelity datasets for ML training in UNDEX-related problems.
- An additional open challenge lies in the strategic exploration of the input parameter space during dataset generation. Due to the high computational cost of full-order simulations, most current studies rely on brute-force or grid-based approaches with limited coverage. However, no systematic effort has yet been made to identify the most informative parameter combinations or to optimize simulation campaigns. In this regard, techniques such as Design of Experiments (DoE) and Active Learning could represent valuable tools. These methods could help reduce the number of required simulations while maximizing the representativeness and informativeness of the training data, particularly for high-dimensional parameter spaces. We identify this as a promising avenue for future investigation.

9 Concluding Remarks

This review has examined the emerging integration of artificial intelligence (AI) and machine learning (ML) into the field of underwater explosion (UNDEX) prediction. Although the body of research is growing rapidly, it remains fragmented and at an early stage of maturity. Three key conclusions emerge:

- **Limited generalizability and realism in current models.** While several ML architectures—including deep neural networks, ensemble methods, and transfer learning—have demonstrated promising results, they are often trained on small, idealized datasets. This severely limits their ability to generalize to real-world naval structures, varying boundary conditions, or full-scale UNDEX scenarios. The lack of physical constraints in many models also raises concerns about prediction reliability.
- **Lack of standardized datasets and robust validation frameworks.** The scarcity of high-fidelity, publicly available datasets remains a major bottleneck. Furthermore, experimental data—crucial for training and validating ML models—are difficult to obtain due to cost and safety constraints. This necessitates a shift toward collaborative dataset generation, shared benchmarks, and rigorous cross-validation protocols.
- **Physics-informed learning and hybrid approaches are the future.** The field must move beyond black-box models toward frameworks that embed physical laws, enable interpretability (e.g., SHAP values), and can adapt across a wide range of geometries and loading conditions. The fusion of simulation, experimental knowledge, and data-driven models will be essential for developing trustworthy, scalable, and application-ready ML solutions for UNDEX.

In sum, while significant challenges remain, the integration of ML into UNDEX analysis holds transformative potential. This review provides a structured foundation for advancing the field toward more efficient, intelligent, and practically deployable prediction systems.

This review has comprehensively analyzed the application of artificial intelligence (AI) and machine learning (ML) techniques for underwater explosion (UNDEX) predictions, highlighting the rapid yet fragmented growth of this research area. While several promising models, including deep neural networks, ensemble methods, and transfer learning strategies, have been developed, a critical examination reveals that current efforts often suffer from significant limitations. These include the scarcity of extensive, high-fidelity datasets, the limited generalizability of models across varying scenarios, and the frequent lack of physically consistent predictions. Moreover, the majority of studies still focus on idealized cases, rarely addressing the complexities of real-world naval structures or operational conditions. Despite these challenges, the advances achieved so far confirm the transformative potential of ML to complement traditional numerical and experimental approaches, enabling faster and more adaptive analyses. Future research must prioritize

the development of standardized datasets, explore physics-informed ML paradigms, and establish robust validation protocols against experimental data to ensure the credibility and applicability of ML-based UNDEX prediction systems. While the field is still maturing, it holds significant promise for reshaping underwater explosion analysis through more efficient, scalable, and interpretable solutions. In conclusion, this review offers a solid foundation for researchers aiming to deepen their understanding of AI-driven modeling in UNDEX scenarios and outlines several promising directions for future investigation to bridge the gap between current research and practical, real-world applications.

Acknowledgements The author(s) disclosed receipt of the following financial support for the research, authorship, and/or publication of this article.

Author Contributions Jacopo Bardiani: Conceptualization, Methodology, Validation, Formal Analysis, Investigation, Data curation, Writing—original draft preparation, Writing—review and editing, Visualization. Claudio Sbarufatti: Methodology, Resources, Writing—review and editing, Supervision. Andrea Manes: Conceptualization, Methodology, Resources, Writing—review and editing, Supervision. All authors have read and agreed to the published version of the manuscript.

Funding Open access funding provided by Politecnico di Milano within the CRUI-CARE Agreement.

Data Availability The data given in this article are the data supporting the results of this study are available upon request.

Declarations

Conflict of interest The authors declare that they have no conflicts of interest relevant to the content of this article.

References

1. Tran P, Wu C, Saleh M, Bortolan Neto L, Nguyen-Xuan H, Ferreira AJM (2021) Composite structures subjected to underwater explosive loadings: a comprehensive review. Compos Struct 268:113684. https://doi.org/10.1016/j.compstruct.2021.113684
2. Ming FR, Zhang AM, Xue YZ, Wang SP (2016) Damage characteristics of ship structures subjected to shockwaves of underwater contact explosions. Ocean Eng 117:359–382. https://doi.org/10.1016/j.oceaneng.2016.03.040
3. de Camargo FV (2019) Survey on experimental and numerical approaches to model underwater explosions. J Mar Sci Eng 7(1):15. https://doi.org/10.3390/jmse7010015
4. Cui P, Zhang AM, Wang SP (2016) Small-charge underwater explosion bubble experiments under various boundary conditions. Phys Fluids. https://doi.org/10.1063/1.4967700
5. Wang H, Cheng YS, Liu J, Gan L (2016) The fluid–solid interaction dynamics between underwater explosion bubble and corrugated sandwich plate. Shock Vib 2016:6057437. https://doi.org/10.1155/2016/6057437
6. Chen S, Qin J, Meng X, Wen Y, Huang R (2023) Numerical simulation research on characteristics of underwater explosive bubble jet in offshore water. J Phys Conf Ser 2478(7):072033. https://doi.org/10.1088/1742-6596/2478/7/072033
7. Yu J, Liu J, He B, Li H, Xie T, Pei D (2021) Numerical research of water jet characteristics in underwater explosion based on compressible multicomponent flows. Ocean Eng 242:110135. https://doi.org/10.1016/j.oceaneng.2021.110135
8. Liu YL, Zhang AM, Tian ZL, Wang SP (2018) Numerical investigation on global responses of surface ship subjected to underwater explosion in waves. Ocean Eng 161:277–290. https://doi.org/10.1016/j.oceaneng.2018.04.094
9. Löhner R, Li L, Soto OA, Baum JD (2023) An arbitrary Lagrangian-Eulerian method for fluid–structure interactions due to underwater explosions. Int J Numer Methods Heat Fluid Flow 33(6):2308–2349. https://doi.org/10.1108/HFF-08-2022-0502
10. Zhang AM, Wu WB, Liu YL, Wang QX (2017) Nonlinear interaction between underwater explosion bubble and structure based on fully coupled model. Phys Fluids. https://doi.org/10.1063/1.4999478
11. Liang CC, Tai YS (2006) Shock responses of a surface ship subjected to noncontact underwater explosions. Ocean Eng 33(5–6):748–772. https://doi.org/10.1016/j.oceaneng.2005.03.011
12. Ramajeyathilagam K, Vendhan CP (2004) Deformation and rupture of thin rectangular plates subjected to underwater shock. Int J Impact Eng 30(6):699–719. https://doi.org/10.1016/j.ijimpeng.2003.01.001
13. Wanchoo P, Matos H, Rousseau CE, Shukla A (2021) Investigations on air and underwater blast mitigation in polymeric composite structures—a review. Compos Struct 263:113530. https://doi.org/10.1016/j.compstruct.2021.113530
14. Yu J, Liu JH, Wang HK, Wang J, Zhou ZT, Mao HB (2022) Application of two-phase transition model in underwater explosion cavitation based on compressible multiphase flows. AIP Adv 12:015316. https://doi.org/10.1063/5.0077517
15. Zhang ZF, Wang C, Wang LK, Zhang AM, Silberschmidt VV (2018) Underwater explosion of cylindrical charge near plates: analysis of pressure characteristics and cavitation effects. Int J Impact Eng 121:91–105. https://doi.org/10.1016/j.ijimpeng.2018.06.009
16. Chahine GL, Kapahi A, Choi JK, Hsiao CT (2016) Modeling of surface cleaning by cavitation bubble dynamics and collapse. Ultrason Sonochem 29:528–549. https://doi.org/10.1016/j.ultsonch.2015.04.026
17. Hsiao CT, Chahine GL (2015) Dynamic response of a composite propeller blade subjected to shock and bubble pressure loading. J Fluids Struct 54:760–783. https://doi.org/10.1016/j.jfluidstructs.2015.01.012
18. Ma J, Hsiao CT, Chahine GL (2015) Modelling cavitating flows using an Eulerian-Lagrangian approach and a nucleation model. J Phys Conf Ser 656(1):012160. https://doi.org/10.1088/1742-6596/656/1/012160
19. Shende S, Nguyen H, Bazilevs Y (2025) Isogeometric analysis of underwater explosion fluid–structure interaction

(UNDEX-FSI). Comput Mech. https://doi.org/10.1007/s00466-025-02607-3
20. Nguyen VT, Phan TH, Duy TN, Park WG (2021) Numerical modeling for compressible two-phase flows and application to near-field underwater explosions. Comput Fluids 215:104805. https://doi.org/10.1016/j.compfluid.2020.104805
21. Cole RH, Weller R (1948) Underwater explosions. Phys Today 1:35. https://doi.org/10.1063/1.3066176
22. Nayak S, Lyngdoh GA, Shukla A, Das S (2022) Predicting the near field underwater explosion response of coated composite cylinders using multiscale simulations, experiments, and machine learning. Compos Struct 283:115157. https://doi.org/10.1016/j.compstruct.2021.115157
23. Keil AH (1961) The response of ships to underwater explosion. SNAME 69:366–410
24. Bardiani J, Lomazzi L, Sbarufatti C, Manes A (2025) A machine learning-based tool to correlate coupled and uncoupled numerical simulations for submerged plates subjected to underwater explosions. J Mar Sci Appl. https://doi.org/10.1007/s11804-025-00624-5
25. Bardiani J, Kyaw Oo D'Amore G, Sbarufatti C, Manes A (2025) Machine learning combined with numerical simulations: an effective way to reconstruct the detonation point of contact underwater explosions with seabed reflection. J Mar Sci Eng 13(3):526. https://doi.org/10.3390/jmse13030526
26. Qiankun J, Gangyi D (2011) A finite element analysis of ship sections subjected to underwater explosion. Int J Impact Eng 38(7):558–566. https://doi.org/10.1016/j.ijimpeng.2010.11.005
27. Ge L, Zhang AM, Wang SP (2020) Investigation of underwater explosion near composite structures using a combined RKDG-FEM approach. J Comput Phys 404:109113. https://doi.org/10.1016/j.jcp.2019.109113
28. Biglarkhani M, Sadeghi K (2017) Incremental explosive analysis and its application to performance-based assessment of stiffened and unstiffened cylindrical shells subjected to underwater explosion. Shock Vib 2017:3754510. https://doi.org/10.1155/2017/3754510
29. Bardiani J, Sbarufatti C, Manes A (2025) Transfer learning with deep neural network toward the prediction of the mass of the charge in underwater explosion events. J Mar Sci Eng 13(2):190. https://doi.org/10.3390/jmse13020190
30. Nowak PR, Szlachta A, Gajewski T, Peksa P, Sielicki PW (2023) Small-scale underwater explosion in shallow-water tank. Ocean Eng 288:115894. https://doi.org/10.1016/j.oceaneng.2023.115894
31. Costanzo FA (2011) Simple tools for simulating structural response to underwater explosions. In: Rotating machinery, structural health monitoring, shock and vibration, volume 5: proceedings of the 29th IMAC, a conference on structural dynamics. Springer, New York, pp 481–498. https://doi.org/10.1007/978-1-4419-9428-8_40
32. Sone Oo YP, Le Sourne H, Dorival O (2020) On the applicability of Taylor's theory to the underwater blast response of composite plates. Int J Impact Eng 145:103677. https://doi.org/10.1016/j.ijimpeng.2020.103677
33. Zhang QL, Huang XY, Li Z (2021) Coupled acoustic-structural analysis of a partially submerged circular RC column in an underwater explosion event: factors to be considered for loading. Ocean Eng 232:109122. https://doi.org/10.1016/j.oceaneng.2021.109122
34. Jin Z, Yin C, Chen Y, Hua H (2017) Coupling Runge-Kutta discontinuous Galerkin method to finite element method for compressible multi-phase flow interacting with a deformable sandwich structure. Ocean Eng 130:597–610. https://doi.org/10.1016/j.oceaneng.2016.12.013
35. Zong Z, Zhao Y, Li H (2013) A numerical study of whole ship structural damage resulting from close-in underwater explosion shock. Mar Struct 31:24–43. https://doi.org/10.1016/j.marstruc.2013.01.004
36. Zhang X, He Z, Du Z, Wang J, Jiang Y, Li Y (2023) Multi-peak phenomenon of large-scale hull structural damage under near-field underwater explosion. Ocean Eng 283:114898. https://doi.org/10.1016/j.oceaneng.2023.114898
37. Ren SF, Zhao PF, Wang SP, Liu YZ (2022) Damage prediction of stiffened plates subjected to underwater contact explosion using the machine learning-based method. Ocean Eng 266:112839. https://doi.org/10.1016/j.oceaneng.2022.112839
38. Liu YZ, Ren SF, Zhao PF (2022) Application of the deep neural network to predict dynamic responses of stiffened plates subjected to near-field underwater explosion. Ocean Eng 247:110537. https://doi.org/10.1016/j.oceaneng.2022.110537
39. Kong XS, Gao H, Jin Z, Zheng C, Wang Y (2023) Predictions of the responses of stiffened plates subjected to underwater explosion based on machine learning. Ocean Eng 283:115216. https://doi.org/10.1016/j.oceaneng.2023.115216
40. Ding P, Buijk A (2006) Simulation of underwater explosion using MSC Dytran. Ann Arbor 1001:48105
41. Liu Y, Li Z, Sun Q, Fan X, Wang W (2013) Separation dynamics of large-scale fairing section: a fluid–structure interaction study. Proc Inst Mech Eng G J Aerosp Eng 227(11):1767–1779. https://doi.org/10.1177/0954410012462317
42. Li J, Rong JL (2012) Experimental and numerical investigation of the dynamic response of structures subjected to underwater explosion. Eur J Mech B-Fluids 32:59–69. https://doi.org/10.1016/j.euromechflu.2011.09.009
43. Wei X, Tran P, De Vaucorbeil A, Ramaswamy RB, Latourte F, Espinosa HD (2013) Three-dimensional numerical modeling of composite panels subjected to underwater blast. J Mech Phys Solids 61(6):1319–1336. https://doi.org/10.1016/j.jmps.2013.02.007
44. Mouritz AP (1995) The effect of underwater explosion shock loading on the fatigue behaviour of GRP laminates. Compos 26(1):3–9. https://doi.org/10.1016/0734-743X(95)00034-8
45. Schiffer A, Tagarielli VL (2015) The response of circular composite plates to underwater blast: experiments and modelling. J Fluids Struct 52:130–144. https://doi.org/10.1016/j.jfluidstructs.2014.10.009
46. Wang H, Liu B, Lei J, Zhao N (2024) Improved deep neural network for predicting structural response of stiffened cylindrical shells to far-field underwater explosion. Ocean Eng 298:117258. https://doi.org/10.1016/j.oceaneng.2024.117258
47. Marchesi G, Bardiani J, Lomazzi L, Manes A (2025) Dimensional analysis and scalability of a simplified hull girder subjected to underwater explosion shock loading. Int J Impact Eng. https://doi.org/10.1016/j.ijimpeng.2025.105332
48. Sigrist JF, Broc D (2023) A versatile method to calculate the response of equipment mounted on ship hulls subjected to underwater shock waves. Finite Elem Anal Des 218:103917. https://doi.org/10.1016/j.finel.2023.103917
49. Bardiani J, Giglio M, Sbarufatti C, Manes A (2025) On the exploration of the influence of seabed reflected waves on naval structures. Eng Proc 85(1):7. https://doi.org/10.3390/engproc2025085007
50. Kim JH, Shin HC (2008) Application of the ALE technique for underwater explosion analysis of a submarine liquefied oxygen tank. Ocean Eng 35(8–9):812–822. https://doi.org/10.1016/j.oceaneng.2008.01.019
51. Yu Z, Ni BY, Wu Q, Wang Z, Liu P, Xue Y (2023) Numerical simulation of icebreaking by underwater-explosion bubbles and compressed-gas bubbles based on the ALE method. J Mar Sci Eng 12(1):58. https://doi.org/10.3390/jmse12010058

52. Liu WT, Ming FR, Zhang AM, Miao XH, Liu YL (2018) Continuous simulation of the whole process of underwater explosion based on Eulerian finite element approach. Appl Ocean Res 80:125–135. https://doi.org/10.1016/j.apor.2018.08.016
53. den Abeele F, Verleysen P (2013) Finite element analysis of subsea pipelines subjected to underwater explosion. In: Proc Int Conf Offshore Mech Arctic Eng (OMAE), vol 2. https://doi.org/10.1115/OMAE2013-10736
54. Jen CY (2009) Coupled acoustic-structural response of optimized ring-stiffened hull for scaled down submerged vehicle subject to underwater explosion. Theor Appl Fract Mech 52:96–110. https://doi.org/10.1016/j.tafmec.2009.08.006
55. Moradloo AJ, Adib A, Pirooznia A (2019) Damage analysis of arch concrete dams subjected to underwater explosion. Appl Math Model 75:709–734. https://doi.org/10.1016/j.apm.2019.04.064
56. Smith M (2009) ABAQUS/standard user's manual, version 6.9. Dassault Systèmes Simulia Corp
57. Wang Y, Dong H, Dong T, Xu X (2022) Dumbbell-shaped damage effect of closed cylindrical shell subjected to far-field side-on underwater explosion shock wave. J Mar Sci Eng 10:1874. https://doi.org/10.3390/jmse10121874
58. Zhou ZH (2021) Machine learning. Springer Nature
59. Brunton SL, Noack BR, Koumoutsakos P (2019) Machine learning for fluid mechanics. Annu Rev Fluid Mech 52:477–508. https://doi.org/10.1146/annurev-fluid-010719-060214
60. Hastie T, Tibshirani R, Friedman J, Franklin J (2005) The elements of statistical learning: data mining, inference and prediction. Math Intell 27(2):83–85. https://doi.org/10.1007/BF02985802
61. Nasrabadi NM (2007) Pattern recognition and machine learning. J Electron Imaging 16(4):049901. https://doi.org/10.1117/1.2819119
62. Jain AK, Mao J, Mohiuddin KM (1996) Artificial neural networks: a tutorial. Computer 29(3):31–44. https://doi.org/10.1109/2.485891
63. Ren S, Chen G, Li T, Chen Q, Li S (2018) A deep learning-based computational algorithm for identifying damage load condition: an artificial intelligence inverse problem solution for failure analysis. Comput Model Eng Sci 117(3):287–307. https://doi.org/10.31614/cmes.2018.04697
64. Karaci A, Yaprak H, Ozkaraca O, Demir I, Simsek O (2018) Estimating the properties of ground-waste-brick mortars using DNN and ANN. Comput Model Eng Sci 118(1):207–228. https://doi.org/10.31614/cmes.2019.04216
65. Guo J, Gu CX, Yang JJ, Zhang Y, Yang H (2020) Data mining and application of ship impact spectrum acceleration based on PNN neural network. Ocean Eng 203:107193. https://doi.org/10.1016/j.oceaneng.2020.107193
66. Lomazzi L, Morin D, Cadini F, Manes A, Aune V (2023) Deep learning-based analysis to identify fluid–structure interaction effects during the response of blast-loaded plates. Int J Prot Struct. https://doi.org/10.1177/20414196231198259
67. Lee T, Kwak BJ, Yu J, Lee JH, Noh Y, Moon YH (2020) Deep-learning approach to predict a severe plastic anisotropy of caliber-rolled Mg alloy. Mater Lett 269:127652. https://doi.org/10.1016/j.matlet.2020.127652
68. Gupta NK (2021) Response of thin-walled metallic structures to underwater explosion: a review. Int J Impact Eng 156:103950. https://doi.org/10.1016/j.ijimpeng.2021.103950
69. Rajendran R, Narasimhan K (2006) Deformation and fracture behaviour of plate specimens subjected to underwater explosion—a review. Int J Impact Eng 32(12):1945–1963. https://doi.org/10.1016/j.ijimpeng.2005.05.013
70. Li G, Shi D, Wang L, Zhao K (2022) Measurement technology of underwater explosion load: a review. Ocean Eng 254:111383. https://doi.org/10.1016/j.oceaneng.2022.111383
71. Matos H, Galuska M, Javier C, Kishore S, LeBlanc J, Shukla A (2024) A review of underwater shock and fluid–structure interactions. Flow 4:E10. https://doi.org/10.1017/flo.2024.8
72. Zhang R, Xiao W, Yao X et al (2025) Review of research on underwater explosions related to ship damage and stability. J Mar Sci Appl. https://doi.org/10.1007/s11804-025-00633-4
73. Kwon YW, Fox PK (1993) Underwater shock response of a cylinder subjected to a side-on explosion. Comput Struct 46(3):637–646. https://doi.org/10.1016/0045-7949(93)90257-E
74. Kiciński R, Szturomski B (2020) Pressure wave caused by trinitrotoluene (TNT) underwater explosion—short review. Appl Sci (Switz) 10(10):3433. https://doi.org/10.3390/app10103433
75. Shahid U, Munir MR, Shah SJ, Shahdin A, Iqbal MZ (2024) Numerical investigation of pulsating bubble dynamics in shallow and deep-sea underwater explosions. J Ocean Eng Mar Energy. https://doi.org/10.1007/s40722-024-00337-x
76. Rajendran R, Narasimhan K (2001) Damage prediction of clamped circular plates subjected to contact underwater explosion. Int J Impact Eng 25(4):373–386. https://doi.org/10.1016/S0734-743X(00)00051-8
77. Geers TL, Hunter KS (2002) An integrated wave-effects model for an underwater explosion bubble. J Acoust Soc Am 111(4):1584–1601. https://doi.org/10.1121/1.1458590
78. Hu H, Li D, Zheng J, Duan C, Zhang Z (2024) Experimental and numerical study on bubble pulsation characteristics of underwater explosions with multiple charges. Phys Fluids. https://doi.org/10.1063/5.0218992
79. Li H, Zhang C, Zheng X, Mei Z, Bai X (2021) A simplified theoretical model of the whipping response of a hull girder subjected to underwater explosion considering the damping effect. Ocean Eng 239:109831. https://doi.org/10.1016/j.oceaneng.2021.109831
80. Chung J, Seo Y, Shin YS (2020) Dynamic and whipping response of the surface ship subjected to underwater explosion: experiment and simulation. Ships Offshore Struct 15(10):1129–1140. https://doi.org/10.1080/17445302.2019.1706924
81. Ghoshal R, Mitra N (2018) Underwater oblique shock wave reflection. Phys Rev Fluids 3(1):013403. https://doi.org/10.1103/PhysRevFluids.3.013403
82. Ghoshal R, Mitra N (2016) Underwater explosion induced shock loading of structures: influence of water depth, salinity and temperature. Ocean Eng 126:22–28. https://doi.org/10.1016/j.oceaneng.2016.08.019
83. Walters AP, Didoszak JM, Kwon YW (2013) Explicit modeling of solid ocean floor in shallow underwater explosions. Shock Vib 20:189–197. https://doi.org/10.3233/SAV-2012-0737
84. Xu LY, Wang SP, Liu YL, Zhang AM (2021) Numerical simulation on the whole process of an underwater explosion between a deformable seabed and a free surface. Ocean Eng 219:108311. https://doi.org/10.1016/j.oceaneng.2020.108311
85. Gannon L (2019) Simulation of underwater explosions in close-proximity to a submerged cylinder and a free-surface or rigid boundary. J Fluids Struct 87:189–205. https://doi.org/10.1016/j.jfluidstructs.2019.03.019
86. Clarke JF (2002) Handbook of shock waves, volumes 1, 2, and 3. Edited by G. Ben-Dor, O. Igra & T. Elperin. Academic, 2001. 889, 792 and 421 pp. ISBN 012 086430 4. J Fluid Mech 453:439–443. https://doi.org/10.1017/S0022112002217693
87. Yu J, Liu JH, Wang HK, Wang J, Zhang LP, Liu GZ (2021) Numerical simulation of underwater explosion cavitation characteristics based on phase transition model in compressible multicomponent fluids. Ocean Eng 240:109934. https://doi.org/10.1016/j.oceaneng.2021.109934

88. Yu J, Zhang XP, Hao Y, Chen JP, Xu YQ (2024) Study on dynamic characteristics of cavitation in underwater explosion with large charge. Sci Rep 14(1):8580. https://doi.org/10.1038/s41598-024-58622-6
89. Sagar HJ, El Moctar O (2023) Dynamics of a cavitation bubble between oblique plates. Phys Fluids. https://doi.org/10.1063/5.0132098
90. Grosan C, Abraham A, Jain LC, Kacprzyk J (2011) Intelligent systems. Springer, Berlin 17:261–268. https://doi.org/10.1007/978-3-642-21004-4
91. Young YL, Liu Z, Xie W (2009) Fluid-structure and shock-bubble interaction effects during underwater explosions near composite structures. ASME J Appl Mech 76(5):051303. https://doi.org/10.1115/1.3129718
92. Avachat S, Zhou M (2016) Compressive response of sandwich plates to water-based impulsive loading. Int J Impact Eng 93:196–210. https://doi.org/10.1016/j.ijimpeng.2016.03.007
93. Avachat S, Zhou M (2012) Effect of facesheet thickness on dynamic response of composite sandwich plates to underwater impulsive loading. Exp Mech 52:83–93. https://doi.org/10.1007/s11340-011-9538-4
94. Koli S, Chellapandi P, Rao LB, Sawant A (2020) Study on JWL equation of state for the numerical simulation of near-field and far-field effects in underwater explosion scenario. Eng Sci Technol Int J 23(4):758–768. https://doi.org/10.1016/j.jestch.2020.01.007
95. Huang M, Yao C, Wang P, Cheng L, Ying W (2025) Physics-informed data-driven cavitation model for a specific Mie-Grüneisen equation of state. J Comput Phys 524:113703. https://doi.org/10.1016/j.jcp.2024.113703
96. Hjelmstad KD (2007) Fundamentals of structural mechanics. Springer Sci Bus Media
97. Bakroon M, Daryaei R, Aubram D, Rackwitz F (2018) Multi-material arbitrary Lagrangian-Eulerian and coupled Eulerian-Lagrangian methods for large deformation geotechnical problems. In: Numerical methods in geotechnical engineering IX, vol 1. CRC Press, pp 673–681. https://doi.org/10.1201/9780429446931-84
98. LeBlanc J, Shillings C, Gauch E et al (2016) Near field underwater explosion response of polyurea coated composite plates. Exp Mech 56:569–581. https://doi.org/10.1007/s11340-015-0071-8
99. Helenbrook BT, Hrdina J (2018) High-order adaptive arbitrary-Lagrangian–Eulerian (ALE) simulations of solidification. Comput Fluids 167:40–50
100. Huang H, Jiao QJ, Nie JX, Qin JF (2011) Numerical modeling of underwater explosion by one-dimensional ANSYS-AUTODYN. J Energy Mater 29:292–325. https://doi.org/10.1080/07370652.2010.527898
101. Giuliano D, Lomazzi L, Giglio M, Manes A (2023) On Eulerian-Lagrangian methods to investigate the blast response of composite plates. Int J Impact Eng 173:104469. https://doi.org/10.1016/j.ijimpeng.2022.104469
102. Bardiani J, Kyaw Oo D'Amore G, Sbarufatti C, Manes A (2025) Underwater explosion analysis on composite marine structures: a comparison between CEL and UEL methods. J Compos Sci 9(4):177. https://doi.org/10.3390/jcs9040177
103. Kwon YW, Fox PK (1993) Underwater shock response of a cylinder subjected to a side-on explosion. Comput Struct 48(4):637–646
104. Zamyshlyayev BV (1973) Dynamic loads in underwater explosion, AD-757183
105. Liu Y, Zhang A, Tian Z (2014) Approximation of underwater explosion bubble by singularities based on BEM. Ocean Eng 75:46–52. https://doi.org/10.1016/j.oceaneng.2013.11.008
106. Zhang AM, Liu YL (2015) Improved three-dimensional bubble dynamics model based on boundary element method. J Comput Phys 294:208–223. https://doi.org/10.1016/j.jcp.2015.03.049
107. Turing AM (2009) Computing machinery and intelligence. In: Epstein R, Roberts G, Beber G (eds) Parsing the turing test. Springer Netherlands, pp 23–65. https://doi.org/10.1093/mind/LIX.236.433
108. Helal S (2018) The expanding frontier of artificial intelligence. Computer 51(9):14–17. https://doi.org/10.1109/MC.2018.3620976
109. Tanaka I, Rajan K, Wolverton C (2018) Data-centric science for materials innovation. MRS Bull 43:659–663. https://doi.org/10.1557/MRS.2018.205
110. Wei J, Chu X, Sun XY, Xu K, Deng HX, Chen J, Wei Z, Lei M (2019) Machine learning in materials science. InfoMat 1:338–358. https://doi.org/10.1002/INF2.12028
111. Kibrete F, Trzepieciński T, Gebremedhen HS, Woldemichael DE (2023) Artificial intelligence in predicting mechanical properties of composite materials. J Compos Sci 7(9):364. https://doi.org/10.3390/jcs7090364
112. Mulenga TK, Rangappa SM, Siengchin S (2025) Natural fiber composites: a comprehensive review on machine learning methods. Arch Comput Methods Eng. https://doi.org/10.1007/s11831-025-10273-0
113. Guo K, Yang Z, Yu CH, Buehler MJ (2021) Artificial intelligence and machine learning in design of mechanical materials. Mater Horiz 8(4):1153–1172. https://doi.org/10.1039/D0MH01451F
114. Bousmaha R, Hamou RM, Amine A (2022) Automatic selection of hidden neurons and weights in neural networks for data classification using hybrid particle swarm optimization, multi-verse optimization based on Lévy flight. Evol Intell 15:1695–1714. https://doi.org/10.1007/s12065-021-00579-w
115. Bartók AP, De S, Poelking C, Bernstein N, Kermode JR, Csányi G, Ceriotti M (2017) Machine learning unifies the modeling of materials and molecules. Sci Adv. https://doi.org/10.1126/SCIADV.1701816
116. Kumar L, Tummalapalli S, Rathi SC, Murthy LB, Krishna A, Misra S (2023) Machine learning with word embedding for detecting web-services anti-patterns. J Comput Lang 75:101207. https://doi.org/10.1016/j.cola.2023.101207
117. Kibrete F, Trzepieciński T, Gebremedhen HS, Woldemichael DE (2023) Artificial intelligence in predicting mechanical properties of composite materials. J Compos Sci. https://doi.org/10.3390/jcs7090364
118. Li Z, Ma F, Zhu W, Jia X, Li Y, Chen L (2024) Prediction of deformation response of target plate in underwater explosion based on deep learning neural network. J Underwater Unmanned Syst 32(6):1045–1052. https://doi.org/10.11993/j.issn.2096-3920.2024-0069
119. Zhou KW, Ding S, Xie YJ, Shao Y, Zhang ZF (2024) A neural network for the prediction of damage to reinforced cylindrical shells subjected to non-contact underwater explosions. J Phys Conf Ser 2891(6):062007. https://doi.org/10.1088/1742-6596/2891/6/062007
120. Zhang M, Drikakis D, Li L, Yan X (2019) Machine-learning prediction of underwater shock loading on structures. Computation 7(4):58. https://doi.org/10.3390/computation7040058
121. Zhang GF, Ren SF, Zhao PF, Liu YZ, Chen H (2024) Damage prediction of ship cabins subjected to underwater contact explosion by deep neural network with grid search algorithm. Ocean Eng 312:119278. https://doi.org/10.1016/j.oceaneng.2024.119278
122. Kohli H, Agarwal J, Kumar M (2022) An improved method for text detection using Adam optimization algorithm. Glob Transit Proc 3(1):230–234. https://doi.org/10.1016/j.gltp.2022.03.028

123. Ma T, Long J, Liu Y (2024) Prediction model of two underwater explosion sources' explosion shock wave peak pressure based on BP neural network. Trans Beijing Inst Technol 44(3):260–269. https://doi.org/10.15918/j.tbit1001-0645.2023.097
124. He Z, Chen X, Zhang X, Jiang Y, Ren X, Li Y (2025) Damage prediction of hull structure under near-field underwater explosion based on machine learning. Appl Ocean Res 154:104329. https://doi.org/10.1016/j.apor.2024.104329
125. Shuang W, Feng L, Feng M, Si C, Wei Z, Feng H, Qinyi H (2024) A deep learning-based solver for underwater shock response spectrum. J Underwater Unmanned Syst 33:1–7. https://doi.org/10.11993/j.issn.2096-3920.2024-0144
126. Fang X, Li H, Zhang SR, Wang XH, Wang C, Luo XC (2023) A combined finite element and deep learning network for structural dynamic response estimation on concrete gravity dam subjected to blast loads. Def Technol 24:298–313. https://doi.org/10.1016/j.dt.2022.04.012
127. Li L, Gu J, Huang X, Zhong D (2023) Dynamic response prediction of underwater explosive vessel based on LOO-XGBoost model. Neural Comput Appl 35(36):25057–25067. https://doi.org/10.1007/s00521-023-08613-x
128. Chen H, Ren SF, Li SM, Zhang S, Zhang GF (2024) Bubble collapse patterns recognition and flow field prediction based on machine learning. Phys Fluids 36(8):087151. https://doi.org/10.1063/5.0218482
129. Li L, Hu Y, Fang C, You Y, Liu K, Huang S (2020) Dynamic response prediction of underwater explosion vessels. IOP Conf Ser Earth Environ Sci 453(1):012040. https://doi.org/10.1088/1755-1315/453/1/012040
130. Hinton GE, Osindero S, Teh YW (2006) A fast learning algorithm for deep belief nets. Neural Comput 18:1527–1554
131. Kusy M, Kowalski PA (2022) Architecture reduction of a probabilistic neural network by merging k-means and k-nearest neighbour algorithms. Appl Soft Comput 128:109387. https://doi.org/10.1016/j.asoc.2022.109387
132. Jafari S, Yang JH, Byun YC (2024) Optimized XGBoost modeling for accurate battery capacity degradation prediction. Results Eng 24:102786. https://doi.org/10.1016/j.rineng.2024.102786
133. Wu Z, Zhang H, Ye H, Zhang H, Zheng Y, Guo X (2025) PINN enhanced extended multiscale finite element method for fast mechanical analysis of heterogeneous materials. Acta Mech 235:4895–4913. https://doi.org/10.1007/s00707-024-03984-1
134. Leng K, Shankar M, Thiyagalingam J (2024) Zero coordinate shift: whetted automatic differentiation for physics-informed operator learning. J Comput Phys 505:112904. https://doi.org/10.1016/j.jcp.2024.112904
135. L.A.N.L. SESAME (1979) The Los Alamos National Laboratory equation of state database. LA-UR-92-407
136. Liu H, Yan G, Duan Z, Chen C (2021) Intelligent modeling strategies for forecasting air quality time series: a review. Appl Soft Comput 102:106957. https://doi.org/10.1016/j.asoc.2020.106957
137. Machello C, Aghabalaei Baghaei K, Bazli M, Hadigheh A, Rajabipour A, Arashpour M, Mahdizadeh Rad H, Hassanli R (2024) Tree-based machine learning approach to modelling tensile strength retention of fibre reinforced polymer composites exposed to elevated temperatures. Compos Part B Eng. https://doi.org/10.1016/J.COMPOSITESB.2023.111132
138. Breiman L, Friedman J, Olshen RA, Stone CJ (2017) Classification and regression trees. Routledge
139. Liu Z, Wang Z, Chu G, Yao X (2025) Structural deformation prediction of underwater exploded ship hull girder using machine learning. J Mar Sci Appl. https://doi.org/10.1007/s11804-025-00689-2
140. Yankov D, DeCoste D, Keogh E (2006) Ensembles of nearest neighbor forecasts. In: Lect Notes Comput Sci (Including Subser. Lect. Notes Artif. Intell. Lect. Notes Bioinformatics) 4212 LNAI, pp 545–556. https://doi.org/10.1007/11871842_51
141. Lee MK, Lee I (2023) Transfer learning with deep neural network toward the prediction of wake flow characteristics of containerships. J Mar Sci Eng 11(10):1898. https://doi.org/10.3390/jmse11101898
142. Mohammed A, Kora R (2023) A comprehensive review on ensemble deep learning: opportunities and challenges. J King Saud Univ Comput Inf Sci 35(2):757–774. https://doi.org/10.1016/j.jksuci.2023.01.014
143. Gauch E, LeBlanc J, Shukla A (2018) Near field underwater explosion response of polyurea coated composite cylinders. Compos Struct 202:836–852. https://doi.org/10.1016/j.compstruct.2018.04.048
144. Zhu X, Mou JL, Wang H, Zhang ZH (2010) Damage modes of stiffened plates subjected to underwater explosion load. Explosion Shock Waves 30(3):225–231. https://doi.org/10.11883/1001-1455(2010)03-0225-07
145. Praba RS, Ramajeyathilagam K (2020) Numerical investigations on the large deformation behaviour of ring stiffened cylindrical shell subjected to underwater explosion. Appl Ocean Res 101:102262. https://doi.org/10.1016/j.apor.2020.102262
146. He Z, Chen Z, Jiang Y, Cao X, Zhao T, Li Y (2020) Effects of the standoff distance on hull structure damage subjected to near-field underwater explosion. Mar Struct 74:102839. https://doi.org/10.1016/j.marstruc.2020.102839
147. Zhang L, An F, Liu J, Dong Y, Li Y, Feng B (2023) Underwater explosion resistance of air-backed plate with steel and polyurea: effect of polyurea spraying position. Ocean Eng 283:115025. https://doi.org/10.1016/j.oceaneng.2023.115025
148. Li SM, Zhang AM, Cui P, Li S, Liu YL (2023) Vertically neutral collapse of a pulsating bubble at the corner of a free surface and a rigid wall. J Fluid Mech 962:A28. https://doi.org/10.1017/jfm.2023.292
149. Gan N, Liu LT, Yao XL, Wang JX, Wu WB (2021) Experimental and numerical investigation on the dynamic response of a simplified open floating slender structure subjected to underwater explosion bubble. Ocean Eng 219:108308. https://doi.org/10.1016/j.oceaneng.2020.108308
150. Zhu X, Zhang ZH, Liu RQ, Zhu YX (2004) Experimental study on the explosion resistance of cabin near shipboard of surface warship subjected to underwater contact explosion. Explosion Shock Waves 24(2):133–139
151. Vanadit-Ellis W, Davis LK (2010) Physical modeling of concrete gravity dam vulnerability to explosions. In: 2010 International Waterside Security Conference, pp 1–11. https://doi.org/10.1109/WSSC.2010.5730291